HHS Public Access

Author manuscript

Brain Imaging Behav. Author manuscript; available in PMC 2018 October 01.

Published in final edited form as:

Brain Imaging Behav. 2017 October ; 11(5): 1258–1277. doi:10.1007/s11682-016-9589-3.

Mapping Temporo-parietal and Temporo-occipital Cortico-cortical Connections of the Human Middle Longitudinal Fascicle in Subject-Specific, Probabilistic, and Stereotaxic Talairach Spaces

N. Makris[1],[2],[3],[4], **A. Zhu**[2],[5], **G. M. Papadimitriou**[1], **P. Mouradian**[1], **I. Ng**[1], **E. Scaccianoce**[6], **G. Baselli**[6], **F. Baglio**[6], **M. E. Shenton**[2],[5],[8], **Y. Rathi**[1],[2], **B. Dickerson**[1], **E. Yeterian**[7], and **M. Kubicki**[1],[2],[8]

[1]Departments of Psychiatry and Neurology Services, Center for Morphometric Analysis, Center for Neural Systems Investigations, Athinoula A. Martinos Center for Biomedical Imaging, Massachusetts General Hospital, Harvard Medical School, Building 149, 13th Street, Charlestown, Boston, MA, 02129 USA

[2]Psychiatry Neuroimaging Laboratory, Department of Psychiatry, Brigham and Women's Hospital and Harvard Medical School, Boston, MA, 02215 USA

[3]Department of Anatomy and Neurobiology, Boston University School of Medicine, Boston, MA 02215

[4]McLean Hospital, Harvard Medical School (Affiliated School/Hospital) Belmont, MA 02478

[5]VA Boston Healthcare System, Boston, MA, 02130 USA

[6]Department of Bioengineering, Politecnico di Milano, Milano, Italy

[7]Department of Psychology, Colby College, Waterville, ME 04901

[8]Department of Radiology, Brigham and Women's Hospital and Harvard Medical School, Boston, MA, 02215, USA

Abstract

Originally, the middle longitudinal fascicle (MdLF) was defined as a long association fiber tract connecting the superior temporal gyrus and temporal pole with the angular gyrus. More recently its description has been expanded to include all long postrolandic cortico-cortical association connections of the superior temporal gyrus and dorsal temporal pole with the parietal and occipital

Correspondence: Nikos Makris, M.D., Ph.D., Massachusetts General Hospital, Center for Morphometric Analysis, Building 149, 13th Street, Charlestown, MA 02129; Tel: 617-726-5743, Fax: 617-726-5711, nikos@cma.mgh.harvard.edu.

Conflicts of Interest

Nikolaos Makris, Anni Zhu, George Papadimitriou, Palig Mouradian, Wingkwai I. Ng, Elisa Scaccianoce, Giuseppe Baselli, Francesca Baglio, Martha Shenton, Yogesh Rathi, Brad Dickerson, Edward H. Yeterian and Marek Kubicki declare that they have no conflict of interest.

Informed Consent

All procedures followed were in accordance with the ethical standards of the responsible committee on human experimentation (institutional and national) and with the Helsinki Declaration of 1975, and the applicable revisions at the time of the investigation. Informed consent was obtained from all patients for being included in the study.

lobes. Despite its location and size, which makes MdLF one of the most prominent cerebral association fiber tracts, its discovery in humans is recent. Given the absence of a gold standard in humans for this fiber tract, its precise and complete connectivity remains to be determined with certainty. In this study using high angular resolution diffusion MRI (HARDI), we delineated for the first time, six major fiber connections of the human MdLF, four of which are temporo-parietal and two temporo-occipital, by examining morphology, topography, cortical connections, biophysical measures, volume and length in seventy brains. Considering the cortical affiliations of the different connections of MdLF we suggested that this fiber tract may be related to language, attention and integrative higher level visual and auditory processing associated functions. Furthermore, given the extensive connectivity provided to superior temporal gyrus and temporal pole with the parietal and occipital lobes, MdLF may be involved in several neurological and psychiatric conditions such as primary progressive aphasia and other aphasic syndromes, some forms of behavioral variant of frontotemporal dementia, atypical forms of Alzheimer's disease, corticobasal degeneration, schizophrenia as well as attention-deficit/hyperactivity disorder and neglect disorders.

Keywords

DTI/HARDI; Middle longitudinal fascicle/Middle longitudinal fasciculus; Inferior longitudinal fascicle/Inferior longitudinal fasciculus; Parietal lobe; Occipital lobe; Primary Progressive Aphasia; Neurodegenerative disorders

Introduction

Pioneering anatomical and clinical-anatomical correlational studies in the 1800s and 1900s fueled interest in human higher cortical functions (Reil and Autenrieth 1809; Broca 1865; Meynert 1865; Wernicke 1874; Dejerine 1895; Flechsig 1901; Brodmann 1905; Economo 1929; Ludwig and Klingler 1956; Geschwind 1965; Luria 1980). In the experimental domain, anatomical investigations in rhesus monkeys expanded to a great extent our knowledge of primate cortical architectonic connections in the second half of the twentieth century (Pandya and Yeterian 1985; Schmahmann and Pandya 2006). In recent years, the advent of diffusion imaging (DTI) (Le Bihan et al. 1986; Basser et al. 1994) enabled the study of connections in humans, both ex-vivo and, most importantly, in-vivo in a non-invasive fashion. Thus it was not surprising that the possibility of using diffusion imaging rekindled the study of in-vivo association cortico-cortical connectivity and higher brain functions such as language in humans (Makris et al. 1997).

Aware of the methodological limitations of both the DTI/HARDI technique (Basser et al. 1994; Tuch et al. 2002) and experimental animal tracing techniques (Cowan et al. 1972; Mesulam 1978), especially of the former in delineating the origins and terminations of fiber pathways (Makris et al. 1999; Makris et al. 2002a; Makris et al. 1997; Schmahmann and Pandya 2006), pioneers of DTI-based long association cortico-cortical connectivity investigations used the classical descriptions of fiber tracts by Dejerine (1895) to validate DTI results regarding human fiber tract anatomy (Makris 1999; Makris et al. 1997) as well as to extrapolate from known monkey fiber tract anatomy (Makris 1999; Makris et al. 2005;

Makris et al. 2002a; Rilling et al. 2008). Although monkey anatomical connectivity served initially as a solid and useful testbed for DTI studies of human anatomical connectivity, given the cortical architectonic differences and cognitive dissimilarities between the two species, it was also expected that long cortico-cortical association fiber pathways would show significant differences in humans compared to monkeys (Makris et al. 2005) as clearly demonstrated by Rilling and colleagues (2008) using diffusion imaging-based tractographic studies (Lori et al. 2002; Mori et al. 1999).

One discovery in human cortico-cortical long association connectivity that originated by extrapolation from monkey experimental material is that of the middle longitudinal fascicle (MdLF) (Seltzer and Pandya 1984). In monkeys, this fiber tract originates from inferior parietal area PG-Opt (equivalent to human angular gyrus) and terminates in areas TPO, PGA and IPa along the upper bank and depth of the superior temporal sulcus (Seltzer and Pandya 1984). In humans, this long association fiber tract was missed by pioneers of human neuroanatomy of the 19th and 20th centuries (Reil and Autenrieth 1809; Burdach 1822; Meynert 1865; Dejerine 1895; Flechsig 1901; Ludwig and Klingler 1956) and was first demonstrated in the human brain only recently. Whereas a histological pilot study using a single brain suggested the presence of MdLF in humans (Makris 1999), a preliminary DTI study in four living subjects demonstrated its existence in the human brain (Makris et al. 2009). MdLF was originally described as a long association fiber pathway within the white matter of the superior temporal gyrus (STG) connecting the STG and temporal pole (TP) with the ipsilateral angular gyrus in the inferior parietal lobule (Makris et al. 2009). A number of subsequent studies using diffusion MRI tractography (Makris et al. 2013a; Makris et al. 2013b; Men jot de Champfleur et al. 2013; Wang et al. 2013) and fiber microdissection (Maldonado et al. 2013; Martino et al. 2013; Wang et al. 2013) expanded our knowledge of the connections of MdLF in humans, showing additional connections of the STG with several parietal and occipital cortical regions.

In the present study, drawing on the existing literature and our own experience we tested the hypothesis that MdLF in humans interconnects the superior temporal gyrus (STG) and dorsal temporal pole (dorsal TP) with the associative cortical regions of the parietal (namely, the angular, AG and supramarginal, SMG gyri, superior parietal lobule, SPL and precuneus, PCN) and occipital (namely, the cuneus, CN and lateral occipital region, LOCC) lobes. To this end we used a tractographic algorithm that selectively *connected only cortical areas (cortex-to-cortex connections)* and not the white matter underneath them as currently practiced in routine diffusion imaging-based tractographic studies. Furthermore, this study investigated the complete cortico-cortical connectivity of MdLF as currently documented. The results revealed four temporo-parietal and two temporo-occipital cortico-cortical components of this fiber tract in 70 subjects (140 cerebral hemispheres). To our knowledge this is the first study to achieve this goal.

Methods

We used magnetic HARDI-based tractography in 70 human subjects to accomplish three goals: a) to delineate the principal cortical regions of origin and/or termination of MdLF within the temporo-parietal and temporo-occipital cortices, specifically the STG, TP, AG,

SMG, SPL, PCN (temporo-parietal) and CN, LOCC (temporo-occipital); b) to map these six subcomponents of the MdLF, i.e., the superior temporal-angular or STG(MdLF)AG connection, the superior temporal-supramarginal or STG(MdLF)SMG connection, the superior temporal-superior parietal lobule or STG(MdLF)SPL connection, the superior temporal-precuneus or STG(MdLF)PCN connection, the superior temporal-cuneus or STG(MdLF)CN connection and the superior temporal-lateral occipital or STG(MdLF)LOCC connection and determine their relative topography within the MdLF; and c) to generate a database of biophysical parameters, such as FA, AD, RD and volume for STG(MdLF)AG, STG(MdLF)SMG, STG(MdLF)SPL, STG(MdLF)PCN, STG(MdLF)CN and STG(MdLF)LOCC. *Terminology* As in a previous publication (Makris et al. 2013b) we used the following naming convention to identify the six connections of the MdLF. The fiber pathway (MdLF) appears in parentheses with the gray matter structures it connects to on either side. For instance “STG(MdLF)AG” denotes that the “MdLF” fiber tract connects the “STG” and “AG” gray matter regions; in other words the gray matter regions “STG” and “AG” are connected via the “MdLF” fiber pathway. For simplicity, in the term “STG(MdLF)AG”, “STG” includes the dorsal part of temporal pole as well as the superior temporal gyrus. This usage is consistent throughout the text, table and figures.

Subjects

Seventy healthy subjects, 59 males and 11 females, 14 to 55 years of age (age 34 on average) participated in the study. Of these subjects, 68 were right-handed, one was left-handed and one was ambidextrous. None of the subjects presented with a diagnosed neurological disorder or history of alcohol or other drug dependency. Subjects were recruited through newspaper advertisements as part of a larger study, and were ascertained to have no Axis I disorder according to the SCID I/NP the Structural Clinical Interview for DSM Disorders (First et al. 1996). This study was approved by the IRBs of both the VA Boston Healthcare System, Brockton Division, and Brigham and Women’s Hospital. Written informed consent was obtained from all subjects prior to study participation. Thirty-seven of these 70 subjects participated in the primary study published by our group (Makris et al. 2013a), and all 70 participated in another study of ours (Makris et al. 2013b) using different anatomical hypotheses, experimental design and methods of diffusion imaging tractographic analysis.

MRI procedures

All subjects were scanned on a 3T GE Echospeed system (General Electric Medical Systems, Milwaukee, WI) using T1-weighted, T2-weighted and echo planar imaging (EPI) HARDI pulse sequences. The T1-weighted sequence consisted of the following parameters: TR = 7.4 ms, TE = 3 ms, TI = 600, 10° flip angle, 25.6 cm^2 field of view, matrix = 256 × 256. The voxel dimensions were 1 × 1 × 1 mm^3. The T2-weighted acquisition (namely, eXtended Echo Train Acquisition) produced a series of contiguous images with TR = 2500 ms, TE = 80 ms, 25.6 cm^2 field of view, and voxel dimensions of 1 × 1 × 1 mm^3. The HARDI acquisition used a double echo sequence (Alexander et al. 1997; Heid 2000) with an 8-channel coil and ASSET (Array Spatial Sensitivity Encoding Techniques, GE); a SENSE-factor (speed-up) of 2 was used to reduce eddy-current and EPI spatial related distortions. A product GE sequence was modified to accommodate for higher spatial resolution, i.e., a

spatial-spectral pulse was replaced by Fat-Sat suppression pulse, and echo spacing was decreased by 15% to accommodate for more slices per TR. Fifty-one (51) noncollinear diffusion directions with b = 900 and eight baseline scans with b = 0 were acquired. Eighty-five (85) axial slices parallel to the AC-PC (anterior commissure-posterior commissure) line spanning the entire brain (no gap) were collected for each subject. Scan parameters were as follows: TR = 17000 ms, TE = 78 ms, FOV = 24 cm, 144 × 144 encoding steps with slice thickness = 1.7 mm, producing isotropic 1.7×1.7×1.7 mm^3 voxels. Total scanning time for the HARDI sequence was 17 minutes. Diffusion data were prepared by removing motion and eddy current artifacts from the raw data using software based on FSL (http://www.fmrib.ox.ac.uk/fsl). Noise filtering was done using a one-step recursive LMMSE estimator for signal estimation and noise removal assuming a Rician noise model (Aja-Fernandez et al. 2008). After reconstruction, diffusion-weighted images were transferred to a LINUX workstation, on which diffusion tensors were estimated in 3-D Slicer software, and then FA, AD and RD were computed from the primary tensor oriented along the fiber tract at each voxel.

Cortical parcellation of temporal, parietal and occipital regions

To define the cortical ROIs in the temporal, parietal and occipital cortices, namely the STG, TP for temporal, AG, SMG, SPL and PCN for parietal, and CN and LOCC for occipital, we carried out analyses using algorithms in the publicly available FreeSurfer software package (http://www.martinos.org/freesurfer) (Dale et al. 1999; Fischl and Dale 2000; Fischl et al. 2002; Fischl et al. 1999; Fischl et al. 2004; Dale et al. 2000). The T1-weighted images from each subject were motion-corrected, averaged, and normalized for intensity; subsequently, automated computational reconstruction of brain surface and segmentation of the cortical and subcortical structures was done. Finally, segmentation and automatic labeling of cortical (i.e., cortical parcellation) and subcortical regions (Desikan et al. 2006; Fischl et al. 2002) were done by implementing algorithms as described by Fischl and colleagues (Dale et al. 1999; Fischl and Dale 2000; Fischl et al. 1999). All ROIs identified in our hypotheses, i.e., STG, TP, AG, SMG, SPL, PCN, CN and LOCC, were characterized using these methods.

Tractographic delineation of MdLF

HARDI tractography was performed in 3D-Slicer (v2.7, www.slicer.org), using a multi-tensor tractography algorithm (Malcolm et al. 2010). This algorithm uses tractography to drive the local fiber model estimation, i.e., model estimation (in this case, the multiple tensors) is done while tracing a “fiber” from seed to termination. It must be pointed out that “fiber” is a computational term used throughout this study to denote “virtual fibers”. Because existing techniques independently estimate the model parameters at each voxel (throughout the brain) prior to tractography, there is no running knowledge of confidence in the estimated model fit. Furthermore, noise can significantly affect the estimated model parameters particularly in the case of multi-tensor models, which others including Malcolm and colleagues (2010) and Baumgartner and colleagues (Baumgartner et al. 2012) have compared with existing methods. Malcolm and colleagues (Malcolm et al. 2010) describe an algorithm that formulates fiber tracking as a recursive estimation process, wherein the estimate at each step of tracing the fiber is guided by those previous estimates. In this model, tractography is performed within a filter framework that uses a discrete mixture of Gaussian

tensors to model the signal. Starting from a seed point, each fiber is traced to its termination using an unscented Kalman filter to simultaneously fit the local model to the signal and propagate it in the most consistent direction. Despite the presence of noise and uncertainty, this method provides a causal estimate of the local structure at each point along the fiber. Furthermore, because each iteration begins with a near-optimal solution based on the previous estimation, the convergence of model fitting is improved and local minima are naturally avoided. Another important aspect of this algorithm is that it provides a measure of confidence (a covariance matrix) in the estimation of the parameters at each step, which can remove false positives in tractography. This approach reduces signal reconstruction error and significantly improves the angular resolution at crossings and branchings. Because it enables detection of two eigenvalues in a voxel, this method resolves the problem of crossing fibers, allowing fiber tracing in areas known to contain such crossing and branching (Rathi et al. 2010). White matter voxels in the brain (FA > 0.15) were used as seed points for (whole-brain) tractography. We then obtained six different fiber tracts for each hemisphere by selecting only the fibers that passed through specific regions for each MdLF connection. All six fiber tracts included the following regions: cortex of the superior temporal gyrus (STG), temporal pole (TP), and a white matter ROI within STG. To generate each individual fiber tract we used the above ROIs with the addition of one of the six cortical ROIs, in the parietal or the occipital lobe. For example, for the generation of STG(MdLF)AG the cortex of the angular gyrus (AG) was included in the analysis with STG, TP and the STG white matter ROI. Thus all six fiber tracts - STG(MdLF)AG, STG(MdLF)SMG, STG(MdLF)SPL, STG(MdLF)PCN, STG(MdLF)CN, and STG(MdLF)LOCC - were delineated using this approach (Figures 1 and 2).

Whereas the cortical ROIs in the STG, TP, AG, SMG, SPL, PCN, CN and LOCC were determined automatically using FreeSurfer, as noted previously, the STG white matter ROI was defined manually. Specifically, this ROI was set by sampling all voxels within the white matter of the STG in a single coronal section in the rostral one-third of the STG, precisely 17 mm caudal to the frontotemporal junction (FTJ), as shown in Figure 1. It is important to note that FTJ corresponds to Y = +4 mm in the rostrocaudal dimension of the Talairach coordinate space system. Given that the STG spans +4 mm to −55 mm in the Talairach Y rostrocaudal dimension, the white matter STG ROI is located approximately at Y = −13 mm and thus within the rostral one-third of STG in Talairach space. This is important for assuring that fibers of the MdLF course through the anterior part of the STG. Therefore, the tractographic approach used in this study had two *necessary* conditions, i.e., specification of the cortical ROIs and the white matter ROI. The first condition for selection of the cortical ROIs ensured that only fibers originating and terminating within these temporal, parietal and occipital cortical regions could be sampled and any fibers passing through their underlying white matter compartment but not entering or exiting these cortices were excluded. Positioning the white matter ROI only within the STG, which also ensured the sampling of all STG white matter voxels in that coronal section, guaranteed that only fibers coursing within the STG were sampled, hence excluding fibers coursing in adjacent regions such as the extreme capsule (EmC) or the middle temporal gyrus. To ensure the anatomical accuracy of MdLF reconstructions, all cases were inspected and all neighboring long association fiber tracts were delineated in five brains by one of the authors (NM) using procedures previously

described by our group (Makris et al. 2005; Makris and Pandya 2009; Makris et al. 2002b; Makris et al. 2009; Makris et al. 2007b; Makris et al. 2013a). Differentiating the MdLF from other fiber tracts such as the EmC, the inferior frontooccipital fascicle (IFOF) and, especially, the arcuate fascicle (AF) is critical (Makris et al. 2013a; Makris et al. 2013b). The distinct trajectories and topographic relationships of MdLF, AF, EmC, IFOF and other long association fiber pathways are shown in detail in Figure 3A. The two *necessary* conditions set in this method help to ensure the exclusion of EmC, IFOF and AF fibers.

Probabilistic Mapping of MdLF

We generated probability maps for STG(MdLF)AG, STG(MdLF)SMG, STG(MdLF)SPL, STG(MdLF)PCN, STG(MdLF)CN and STG(MdLF)LOCC in MNI152 standard space (Evans et al. 1993) by first registering each subject to an MNI152 template with a resolution of 1 mm^3. The FA map of each subject was registered linearly using FLIRT (Jenkinson and Smith 2001), and then nonlinearly using ANTS (Avants et al. 2008). We then applied the same deformation to the fiber tracts to set them in MNI152 space and calculated a fiber tract mask on the MNI152 template for each subject. In this mask a voxel has a value only if a tract traverses it. Finally, to obtain the probabilistic maps, we averaged the masks of all subjects. Furthermore, we computed probabilistic maps of average (across individuals) tract representations overlaid onto the MNI template brain. The tract terminations of each MdLF branch were projected on the inflated brain surface (generated using FreeSurfer) of the MNI brain.

Quantitative Analyses

Measurements of volume, length, mean FA, mean AD and mean RD of six subdivisions of the left and the right MdLF were obtained in all 70 subjects (140 middle longitudinal fascicles). The DTI biophysical parameters of FA, AD and RD may relate to fiber tract coherence and integrity (Basser 2004; Song et al. 2003; Song et al. 2002). *Symmetry index (SI)* (SI = (Left— Right) / 0.5 (Left + Right) (Galaburda et al. 1987) for left and right MdLF for measures of volume, mean FA, mean AD and mean RD were calculated for each individual, and across subjects.

Results

Tracing of MdLF, its Differentation from Adjacent Fiber Tracts and Quantitative Results

As in previous studies, we differentiated the MdLF from other neighboring fiber tracts such as the AF, SLFII, SLFIII (Makris et al. 2005), EmC (Makris and Pandya 2009) and IFOF (Makris et al. 2013b) as shown in Figure 3A. We further differentiated MdLF from ILF, given their close topographical relationship as shown in Figure 3B. Furthermore, the delineation of the STG(MdLF)AG, STG(MdLF)SMG, STG(MdLF)SPL, STG(MdLF)PCN, STG(MdLF)CN and STG(MdLF)LOCC connections within the MdLF were determined tractographically (Figure 4A, B). With a sample of 70 normal subjects, this is the largest study for all six subcomponents of MdLF according to our previous data (Makris et al. 2013a). STG(MdLF)AG connections were acquired on the left in 41(59%) subjects and on right in 39(56%) subjects. STG(MdLF)SMG connections were acquired on the left in 37(53%) subjects and on the right in 32(46%), STG(MdLF)SPL connections were acquired

on the left in 36(51%) subjects and on the right in 35(49.3%) subjects. STG(MdLF)PCN was acquired on the left in 35(50.7%) subjects and on the right in 35(50%) subjects. STG(MdLF)CN was acquired on the left in 1(1.4%)subject, and on the right in 6 (8.6%)subjects. Finally, the STG(MdLF)LOCC was acquired on the left in 17(24%) subjects and on the right in 24(34%) subjects. Table 1 shows the volumes, length, mean FA, mean AD, and mean RD of the left and right STG(MdLF)AG, STG(MdLF)SMG, STG(MdLF)SPL, STG(MdLF)PCN, STG(MdLF)CN, and STG(MdLF)LOCC. The overall mean volume of MdLF was 5.475 cm^3 (5.23 cm^3 on the left, and 5.72 cm^3 on the right). The lengths of MdLF's six connections have different ranges, from approximately 6.85 cm to 10 cm spanning from the parietal and occipital lobes to the temporal pole. Figure 5 shows the same results as Table 1 graphically.

Mapping of STG(MdLF)AG, STG(MdLF)SMG, STG(MdLF)SPL, STG(MdLF)PCN, STG(MdLF)CN and STG(MdLF)LOCC

Figure 6 shows a 3-D reconstruction of the MdLF mapped onto a semitransparent 3-D reconstruction of the MNI brain. This reconstruction represents the MdLF tracts of the entire subject population. The 3-D Slicer software environment was used to create these images.

Three-dimensional reconstructions elucidated the relative topography of STG(MdLF)AG, STG(MdLF)SMG, STG(MdLF)SPL, STG(MdLF)PCN, STG(MdLF)CN, and STG(MdLF)LOCC within the MdLF. Within the STG white matter core, STG(MdLF)AG was located ventrally and laterally with respect to STG(MdLF)SPL, which was positioned dorsally and medially, whereas the fibers of the other less prominent fiber tracts remained intertwined within this space. Caudally at the temporo-parietal and temporo-occipital transition of STG the six fiber tracts split and course as separate entities within the parietal and occipital lobes (Figures 3 and 7). STG(MdLF)AG follows a lateral course penetrating the cortex of AG, whereas STG(MdLF)SMG follows a distinct trajectory remaining rostroventral to STG(MdLF)AG. STG(MdLF)SPL courses dorsally and medially with respect to STG(MdLF)AG to enter the cortex of SPL, whereas STG(MdLF)PCN courses medially to STG(MdLF)SPL and enters the cortex of PCN. The two temporo-occipital connections of STG, i.e., STG(MdLF)LOCC and STG(MdLF)CN follow more ventral trajectories with respect to temporo-parietal fiber pathways. Consistent with the mesial location of the cuneus and the position of the lateral occipital cortex in the lateral aspect of the occipital lobe, the STG(MdLF)CN remains medial to the STG(MdLF)LOCC (Figure 7). In addition, we reconstructed these fiber tracts using Talairach coordinates in the MNI standard space (Figure 7). Furthermore, the probabilistic maps of average (across individuals) tract representations overlaid onto the MNI template brain are shown in Figure 8. Additionally, the tract terminations of each MdLF branch are projected on the inflated brain surface (generated using FreeSurfer) of the MNI brain.

Discussion

In this study we delineated six distinct connections within the MdLF in seventy subjects using multi-tensor tractography. Importantly, these connections were cortex-to-cortex connections, specifically between the cortex of the superior temporal gyrus (including the

dorsal part of the temporal pole) and the cortices of the angular gyrus, the supramarginal gyrus, the superior parietal lobule and the precuneus in the parietal lobe, and the cortices of the cuneus and the lateral occipital region in the occipital lobe. We then mapped them in MNI and Talairach standard spaces. Furthermore, we generated a database of volume and length and of biophysical parameters, such as FA, AD and RD, for STG(MdLF)AG, STG(MdLF)SMG, STG(MdLF)SPL, STG(MdLF)PCN, STG(MdLF)CN and STG(MdLF)LOCC.

The scant available literature on MdLF makes the present study the first systematic, quantitative analysis of six specific subcomponents of the human MdLF, of which four are temporo-parietal and two temporo-occipital. This pathway was originally proposed in humans as a long cortico-cortical connection between STG (including the TP) and AG by Makris and colleagues (2009) using DTI tractography in four subjects (eight hemispheres) (Makris et al. 2009), following a hypothesis based on rhesus monkey autoradiographic (Seltzer and Pandya 1984) and preliminary human histological (Makris 1999) data. Since the appearance of MdLF in the mainstream of human neuroanatomical literature in 2009, our understanding of this long association fiber tract has been evolving. The original MdLF connection between the STG and AG in humans has been confirmed by a few neuroimaging studies (Kamali et al. 2014a; Kamali et al. 2014b; Men jot de Champfleur et al. 2013; Turken and Dronkers 2011). Furthermore, the connectivity of MdLF has been expanded to additional postrolandic regions in the superior and medial parietal as well as the lateral and medial occipital lobes using diffusion imaging tractography (Kamali et al. 2014a; Kamali et al. 2014b; Makris et al. 2013a; Men jot de Champfleur et al. 2013; Wang et al. 2013) and fiber microdissection (Maldonado et al. 2013; Martino et al. 2013; Wang et al. 2013). A unifying aspect of these different MdLF connections is that all are long cortico-cortical association fiber tracts that course within the core white matter of the superior temporal gyrus. Given MdLF's morphological and connectional complexity as well as the diversity of methodologies used for its delineation, the definition of this fiber tract has created some confusion (De Witt Hamer et al. 2011; Maldonado et al. 2013; Wang et al. 2013). To help clarify the nature of MdLF in this growing conundrum, a detailed delineation and precise description of each of its connections in terms of origin and termination as well as of its trajectory could be highly relevant. Therefore, the combination of tractography along with a) precise cortical information, as provided by cortical parcellation techniques (Caviness et al. 1996; Desikan et al. 2006; Fischl et al. 2002) and b) unequivocal topographic information by mapping the fiber tracts onto a standard stereotactic space (Evans et al. 1993; Talairach and Tournoux 1988) as implemented in this study and other studies by our group (Makris et al. 2009; Makris et al. 2013a; Makris et al. 2013b), seem two logical requirements of this process. It should be noted that portions of adjacent fiber tracts may occupy some common space along their trajectories, i.e., there can be evident, partial commingling of fibers within a common space or "cloud" as elaborated upon in a recent study by our group (Makris et al. 2015). This is of interest in this study given the apparent communalities that STG(MdLF)LOCC and ILF present even though they are two distinct fiber tracts (Figures 3B, 7D and 8).

Functional roles of subcomponents of MdLF

The cortical areas of origin and termination in the temporal, parietal and occipital lobes of MdLF are associated with a variety of functions and its six subcomponents are a structural part of the networks that carry out these functions. Based on this principle of functional neuroanatomy and in the light of our present results some general comments with respect to the possible functions of MdLF can be made with respect to language, attention and higher level visual and auditory processing. More specifically, *MdLF's possible function in language* stems from the connection of STG with the inferior parietal lobule (AG and SMG), lateralized on the left (Makris et al. 2009; Makris et al. 2013a; Makris et al. 2013b). Interestingly, our results showed a small leftward lateralization for both STG(MdLF)AG (left 59% vs. right 56% of the subjects) and STG(MdLF)SMG (left 53% vs. right 46% of the subjects) connections. More specifically, the STG(MdLF)AG connection could be part of the stream involved in coding of sublexical representations (such as phonemes and syllables) into articulatory forms and in acoustic-phonetic processing of words and word production as suggested in Hickok and Poeppel's model of speech processing (Hickok 2001; Hickok and Poeppel 2000, 2007). By contrast, the STG(MdLF)SMG connection may be involved in phonetic processing as suggested recently by Gow et al. (Gow et al. 2009; Gow et al. 2008) using magnetoencephalography, electroencephalography and MRI. In this model, a feedback association between SMG and posterior STG would account for normalizing posterior STG phonetic representations (Gow et al. 2009). Moreover, a recent study by Mesulam and colleagues (Mesulam et al. 2015) indicated that the left anterior temporal lobe (including the temporal pole) is involved in word and sentence comprehension, which supports MdLF's role in the language network, a notion supported also by functional connectivity work by Kellmeyer et al. (2013). It is of interest to note that the human anterior temporal region is homologous to a similar region of the monkey brain known to be connected with parieto-occipital areas by MdLF (e.g., Seltzer and Pandya 1984; Schmahmann and Pandya 2006). This anterior temporal region in the monkey plays a key role in conspecific auditory communication and is considered part of the "what" (vs. "where") cortical auditory pathway (e.g., Petkov et al. 2008; Rauschecker and Tian 2000; Tian et al. 2001). Another possible functional role of MdLF may be in *visuospatial and attention functions*. This would be ascribed principally to its connection with the right inferior parietal lobule and with the superior parietal lobule bilaterally and the STG(MdLF)SPL connection. SPL is known to code body part location information in a body-centered coordinate system and to establish the relative location of objects with respect to the body (e.g., Duffy and Burchfiel 1971; Lacquaniti et al. 1995; Mountcastle et al. 1975; Sakata et al. 1973) indicating STG(MdLF)SPL's role in visuospatial attention (Suchan et al. 2014; Thiebaut de Schotten et al. 2011). Moreover, SPL along with the AG would play an important role in attention processing, which is a dominant function of the right hemisphere (e.g., Cabeza and Nyberg 2000; Corbetta and Shulman 2002; Critchley 1966; Duncan and Owen 2000; Goldman-Rakic 1988; Heilman et al. 1970; Heilman and Valenstein 1985; Heilman and Van Den Abell 1980; Heilman et al. 1983; Mesulam 1990, 1998; Posner and Petersen 1990). Our current analysis did not reveal a significant lateralization for STG(MdLF)SPL (i.e., left 50.7% vs. right 49.3% of the subjects). Our results indicating a non-significant asymmetry with respect to the STG to IPL connection also suggested the greater relevance of the STG(MdLF)AG and STG(MdLF)SMG connections in the right hemisphere, consistent with the role of the

superior temporal cortex in both monkeys (Watson et al. 1994) and humans (Karnath et al. 2001) in attention processing, which may be as prominent as language in the left hemisphere.

Possible functional role of MdLF in high order auditory and visual association functions

The fibers of MdLF connect with the dorsal part of TP (BA 38), which corresponds roughly to areas TAr and TAp and is rostral to von Economo's area TA (Ding et al. 2009). Area TAr has been shown to be associated with higher order auditory association processing in monkeys (Poremba et al. 2003), whereas area TAp is polysensory association cortex (Bruce et al. 1981; Seltzer and Pandya 1978, 1991) showing responses to both auditory and visual stimuli in monkeys (Poremba et al. 2003). Importantly, it has been shown that SPL is involved in integrative processing of audio-visual multisensory information in humans (Molholm et al. 2006). Thus MdLF connections between the TP and AG, SPL, CN and LOCC could play a role in integrating auditory with visual information.

Clinical implications

Given the extensive connectivity provided by MdLF between the superior temporal gyrus and temporal pole and the entire parietal lobe and the associative cortices of the medial and lateral occipital lobe, this fiber tract may be involved in several neurological and psychiatric conditions. These could include primary progressive aphasia (Mesulam et al. 2015; Sapolsky et al. 2010) and other aphasic syndromes, some forms of the behavioral variant of frontotemporal dementia (bvFTD) (Rascovsky et al. 2011), atypical forms of Alzheimer's disease in which temporoparietal degeneration is relatively focal (Crutch et al. 2013), corticobasal degeneration (Armstrong et al. 2013), schizophrenia (Armstrong et al. 2013; Asami et al. 2013) as well as attention-deficit/hyperactivity disorder (ADHD) and neglect disorders (Heilman and Valenstein 1985; Makris et al. 2007a). *Primary progressive aphasia* and *aphasic syndromes* The MdLF's strong connections between the superior temporal gyrus (including the dorsal temporal pole) and the inferior parietal lobule (angular and supramarginal gyri) seem to be critical components of the language system in the dominant hemisphere (Dejerine 1895; Geschwind and Galaburda 1987), especially for word and sentence comprehension (Mesulam et al. 2015) the breakdown of which is a hallmark of classical Wernicke's aphasia or in semantic logopenic forms of Primary progressive aphasia (Gorno-Tempini et al. 2011). In these aphasia syndromes the involvement of the MdLF may be one of the core neuroanatomical features of the clinical phenotype. *Behavioral variant frontotemporal dementia* Although not usually associated with tracts such as the MdLF, some forms of bvFTD affect primarily the right temporal pole and adjacent structures within the temporal cortex, leading to socioaffective impairments, prosopagnosia, and other person specific multimodal semantic memory impairment (Chan et al. 2009). FTD patients with genetic mutations in granulin (*GRN*) often have lateralized neurodegeneration with much more notable involvement of the posterior temporal and parietal cortex than is typically seen in FTD (Whitwell et al. 2012); these patients likely have substantial involvement of the MdLF and may have substantial topographic disorientation or limb apraxia. Alzheimer's disease (AD) is usually conceptualized as initially affecting medial temporal lobe, retrosplenial cortex, and related circuitry; however, many atypical variants of AD are associated with focal degeneration of the temporoparietal cortex (Wolk et al. 2010).

Posterior cortical atrophy is one such variant (Crutch et al. 2013) as is young-onset AD (Barnes et al. 2015); these patients tend to have less prominent memory loss and more prominent visuospatial symptoms (including Balint's syndrome) or transcortical aphasia syndromes with or without Gerstmann's syndrome (Benson et al. 1988). Corticobasal degeneration is associated with asymmetric rigidity, limb apraxia, alien limb syndrome, myoclonus, and varying degrees of language or visuospatial impairment depending on lateralization; localization tends to feature asymmetric perirolandic neurodegeneration with involvement of inferior parietal lobule (Armstrong et al. 2013). *Schizophrenia* Positive symptoms such as thought disorder and auditory hallucinations have been associated with abnormalities of the left superior temporal gyrus in schizophrenia and it seems that MdLF may be a critical fiber tract in this disorder (Barta et al. 1990; Kasai et al. 2003; Asami et al. 2013; Makris et al. 2010; Rajarethinam et al. 2004). *attention-deficit/hyperactivity disorder and neglect disorders*. The MdLF's strong connections between the superior temporal gyrus and the inferior and superior parietal lobules in the non-dominant hemisphere are important parts of the visuospatial attention system (Heilman and Van Den Abell 1980; Thiebaut de Schotten et al. 2011). Therefore any damage to these connections could result in ADHD (Makris et al. 2007a; Makris et al. 2008) or certain forms of neglect disorders such as hemi-inattention and hemispatial neglect (Heilman and Valenstein 1985).

Quantitative analyses

The volumes, length, mean FA, mean AD, and mean RD of the left and right STG(MdLF)AG, STG(MdLF)SMG, STG(MdLF)SPL, STG(MdLF)PCN, STG(MdLF)CN, and STG(MdLF)LOCC in 70 healthy human subjects are shown in Table 1 and Figure 5. The overall mean volume of MdLF was 5.475 cm^3 (5.23 cm^3 on the left, and 5.72 cm^3 on the right). These values are slightly higher than yet similar to previous observations by our group performed in a smaller number of subjects, in which the overall volume of the MdLF was found to be 4.55 cm^3 (Makris et al. 2009) or 4.125 cm^3 (Makris et al. 2013a). Thus, the present observations corroborate those of our earlier investigation. MdLF occupies approximately 1.27% of total cerebral white matter, which has been estimated to be 432.47 cm^3 (Makris et al. 1999). Compared with other long association fiber tracts, MdLF is a medium size long association fiber bundle. It is roughly the same size as SLF III, smaller than the cingulum bundle and SLF II, and larger than the superior occipitofrontal fascicle (Makris et al. 2007b). The MdLF mean FA was .324 on the left and .340 on the right, similar to the FA reported in a previous study of MdLF (Makris et al. 2009) and in other studies of different fiber tracts in the normal human brain (Klingberg et al. 2000; Pierpaoli and Basser 1996). *Analysis of symmetry* The MdLF showed minor leftward volumetric asymmetry for the STG(MdLF)AG and STG(MdLF)SMG connections, which are language function related on the left. These asymmetries were not statistically significant as was the case for other biophysical parameters such as FA, AD and RD. Given that the MdLF may be functionally involved in language in the left hemisphere but may also play a prominent role in visuospatial attention function in the right hemisphere, it may be that both the left and the right MdLFs are comparably robust, resulting in no significant asymmetry of their biophysical characteristics. In this analysis, we did not observe any significant asymmetry in length.

Limitations and future studies

When interpreting results of this study, a number of limitations should be considered. This sample of 70 normal subjects is the largest so far for MdLF analyses. However, with much larger samples and with higher spatial resolution, we may acquire a more complete understanding of the different connections of MdLF and of their quantitative profiles. Furthermore, given that our results are based on a group containing predominantly males, they should not be considered representative of female MdLF fiber connections. Moreover, although our diffusion data are of high quality and high resolution, the majority of limitations of the methodology still apply, i.e., DTI can lead to topological interpretations that are biased by the anatomical contents of the tissue (i.e., multiple intersecting axons within one voxel) and can misrepresent actual tract anatomy. Besides the limitations inherent to diffusion imaging tractography, another limitation is the lack of an anatomical gold standard in the human brain with respect to the origins and terminations of the long association fiber tracts, a critical fact that has been raised since the beginning of diffusion tensor imaging of human association fiber tracts (Makris et al. 1997). Thus there is currently an abundance of conflicting information regarding the precise anatomy of human cerebral connectivity. Future functional studies using language and attention paradigms and implementing multimodal neuroimaging procedures of functional and structural MRI may elucidate further the role of the different subcomponents of the MdLF in human cognition.

Conclusion

Based on multi-tensor DTI tractographic analysis we delineated and quantified six connections of the superior temporal gyrus (including the dorsal temporal pole) with the parietal and occipital lobes within MdLF in 70 healthy adult volunteers (68 right-handed), the largest population in which this recently discovered human fiber tract has been studied to date. Moving beyond previous studies, we were able to quantify these six subcomponents of MdLF, namely four temporo-parietal and two temporo-occipital. The strongest connections of the MdLF were principally with temporal pole, superior temporal gyrus, angular gyrus, superior parietal lobule and precuneus. Based on the functional roles of the cortical areas that are interconnected, we suggest that the STG(MdLF)AG, and STG(MdLF)SMG, STG(MdLF)SPL, STG(MdLF)PCN connections of the STG with the parietal lobes may be related to language and attention processing. By contrast, the STG(MdLF)CN and STG(MdLF)LOCC connections may play a role in higher order visual processing. Finally, MdLF connections of the anterior temporal region, including TP, with AG, SPL, CN and LOCC, may play a role in integrating auditory with visual information.

Acknowledgments

The authors would like to thank Mr. Yeetzou Kao for excellent editorial assistance.

Funding This study was supported, in part, by grants from: NINDS, R21NS077059 and R21NS079905 (NM and BD); from NIA/NIMH, R01AG042512 (NM); from NIMH, R01 MH102377 (MK and NM); from NIMH, R01MH097979 (YR).

References

Aja-Fernandez S, Niethammer M, Kubicki M, Shenton ME, Westin CF. Restoration of DWI data using a Rician LMMSE estimator. IEEE Trans Med Imaging. 2008; 27(10):1389–1403. DOI: 10.1109/TMI.2008.920609 [PubMed: 18815091]

Alexander AL, Tsuruda JS, Parker DL. Elimination of eddy current artifacts in diffusion-weighted echo-planar images: the use of bipolar gradients. Magn Reson Med. 1997; 38(6):1016–1021. [PubMed: 9402204]

Armstrong MJ, Litvan I, Lang AE, Bak TH, Bhatia KP, Borroni B, et al. Criteria for the diagnosis of corticobasal degeneration. Neurology. 2013; 80(5):496–503. DOI: 10.1212/WNL.0b013e31827f0fd1 [PubMed: 23359374]

Asami T, Saito Y, Whitford TJ, Makris N, Niznikiewicz M, McCarley RW, et al. Abnormalities of middle longitudinal fascicle and disorganization in patients with schizophrenia. Schizophr Res. 2013; 143(2–3):253–259. [PubMed: 23290607]

Avants BB, Epstein CL, Grossman M, Gee JC. Symmetric diffeomorphic image registration with cross-correlation: evaluating automated labeling of elderly and neurodegenerative brain. Med Image Anal. 2008; 12(1):26–41. [PubMed: 17659998]

Barnes J, Dickerson BC, Frost C, Jiskoot LC, Wolk D, van der Flier WM. Alzheimer's disease first symptoms are age dependent: Evidence from the NACC dataset. Alzheimers Dement. 2015; 11(11):1349–1357. DOI: 10.1016/j.jalz.2014.12.007 [PubMed: 25916562]

Barta PE, Pearlson GD, Powers RE, Richards SS, Tune LE. Auditory hallucinations and smaller superior temporal gyral volume in schizophrenia. Am J Psychiatry. 1990; 147(11):1457–1462. [PubMed: 2221156]

Basser PJ. Scaling laws for myelinated axons derived from an electrotonic core-conductor model. J Integr Neurosci. 2004; 3(2):227–244. [PubMed: 15285056]

Basser PJ, Mattiello J, LeBihan D. MR diffusion tensor spectroscopy and imaging. Biophys J. 1994; 66(1):259–267. DOI: 10.1016/S0006-3495(94)80775-1 [PubMed: 8130344]

Baumgartner, C., Michailovich, O., Levitt, J., Pasternak, O., Bouix, S., Westin, C-F., et al. A unified tractography framework for comparing diffusion models on clinical scans. Paper presented at the CDMRI-workshop (MICCAI'12); London, UK. 2012.

Benson DF, Davis RJ, Snyder BD. Posterior cortical atrophy. Arch Neurol. 1988; 45(7):789–793. [PubMed: 3390033]

Broca P. Sur la siege de la faculte du langage articule. Bulletin d' Anthropologie. 1865; 6:377–393.

Brodmann K. Beitrage zur histologischen Lokalisation der Grosshirnrinde. III. Mitteilung. Die Rindenfelder der niederen Affen. J Psychol Neurol. 1905; 4:177–226.

Bruce C, Desimone R, Gross CG. Visual properties of neurons in a polysensory area in superior temporal sulcus of the macaque. J Neurophysiol. 1981; 46(2):369–384. [PubMed: 6267219]

Burdach, CF. Baue und Leben des Gehirns. Leipzig: in der Dyk'schen Buchhandlung; 1822.

Cabeza R, Nyberg L. Neural bases of learning and memory: functional neuroimaging evidence. Curr Opin Neurol. 2000; 13(4):415–421. [PubMed: 10970058]

Caviness VSJ, Makris N, Meyer J, Kennedy D. MRI-based parcellation of human neocortex: an anatomically specified method with estimate of reliability. J Cog Neurosci. 1996; 8(6):566–588.

Chan D, Anderson V, Pijnenburg Y, Whitwell J, Barnes J, Scahill R, et al. The clinical profile of right temporal lobe atrophy. Brain. 2009; 132(Pt 5):1287–1298. DOI: 10.1093/brain/awp037 [PubMed: 19297506]

Corbetta M, Shulman GL. Control of goal-directed and stimulus-driven attention in the brain. Nat Rev Neurosci. 2002; 3(3):201–215. [PubMed: 11994752]

Cowan WM, Gottlieb DI, Hendrickson AE, Price JL, Woolsey TA. The autoradiographic demonstration of axonal connections in the central nervous system. Brain Res. 1972; 37(1):21–51. [PubMed: 4110604]

Critchley M. Is developmental dyslexia the expression of minor cerebral damage? Clin Proc Child Hosp Dist Columbia. 1966; 22(8):213–222. [PubMed: 5231793]

Crutch SJ, Schott JM, Rabinovici GD, Boeve BF, Cappa SF, Dickerson BC, et al. Shining a light on posterior cortical atrophy. Alzheimers Dement. 2013; 9(4):463–465. DOI: 10.1016/j.jalz.2012.11.004 [PubMed: 23274153]

Dale AM, Fischl B, Sereno MI. Cortical surface-based analysis. I. Segmentation and surface reconstruction. Neuroimage. 1999; 9(2):179–194. DOI: 10.1006/nimg.1998.0395 [PubMed: 9931268]

Dale AM, Liu AK, Fischl BR, Buckner RL, Belliveau JW, Lewine JD, et al. Dynamic statistical parametric mapping: combining fMRI and MEG for high-resolution imaging of cortical activity. Neuron. 2000; 26(1):55–67. [PubMed: 10798392]

De Witt Hamer PC, Moritz-Gasser S, Gatignol P, Duffau H. Is the human left middle longitudinal fascicle essential for language? A brain electrostimulation study. Hum Brain Mapp. 2011; 32(6):962–973. [PubMed: 20578169]

Dejerine, J. Anatomie des Centres Nerveux. Paris, France: Rueff et Cie; 1895. 1980, Masson ed

Desikan RS, Segonne F, Fischl B, Quinn BT, Dickerson BC, Blacker D, et al. An automated labeling system for subdividing the human cerebral cortex on MRI scans into gyral based regions of interest. Neuroimage. 2006; 31(3):968–980. DOI: 10.1016/j.neuroimage.2006.01.021 [PubMed: 16530430]

Ding SL, Van Hoesen GW, Cassell MD, Poremba A. Parcellation of human temporal polar cortex: a combined analysis of multiple cytoarchitectonic, chemoarchitectonic, and pathological markers. J Comp Neurol. 2009; 514(6):595–623. [PubMed: 19363802]

Duffy FH, Burchfiel JL. Somatosensory system: organizational hierarchy from single units in monkey area 5. Science. 1971; 172(3980):273–275. [PubMed: 4994137]

Duncan J, Owen AM. Common regions of the human frontal lobe recruited by diverse cognitive demands. Trends Neurosci. 2000; 23(10):475–483. [PubMed: 11006464]

Economo, C. The cytoarchitectonics of the human cerebral cortex. London: Oxford University Press; 1929.

Evans AC, Collins DL, Mills SR, Brown ED, Kelly RL, Peters TM. 3D statistical neuroanatomical model from 305 MRI volumes. Nuclear Science Symposium and Medical Imaging Conference, 1993 IEEE Conference Record. 1993; 3:1813–1817.

First, MB., Spitzer, RL., Gibbon, M., Williams, JBW. Structured Clinical Interview for DSM-IV Axis I Disorders, Clinician Version (SCID-CV). Washington, D.C: American Psychiatric Press, Inc; 1996. DSM-IV.

Fischl B, Dale AM. Measuring the thickness of the human cerebral cortex from magnetic resonance images. Proc Natl Acad Sci U S A. 2000; 97(20):11050–11055. DOI: 10.1073/pnas.200033797 [PubMed: 10984517]

Fischl B, Salat DH, Busa E, Albert M, Dieterich M, Haselgrove C, et al. Whole brain segmentation: automated labeling of neuroanatomical structures in the human brain. Neuron. 2002; 33(3):341–355. [PubMed: 11832223]

Fischl B, Sereno MI, Dale AM. Cortical surface-based analysis. II: Inflation, flattening, and a surface-based coordinate system. Neuroimage. 1999; 9(2):195–207. DOI: 10.1006/nimg.1998.0396 [PubMed: 9931269]

Fischl B, van der Kouwe A, Destrieux C, Halgren E, Segonne F, Salat DH, et al. Automatically parcellating the human cerebral cortex. Cereb Cortex. 2004; 14(1):11–22. [PubMed: 14654453]

Flechsig P. Developmental (myelogenetic) localisation of the cerebral cortex in the human subject. Lancet. 1901; 2:1027–1029.

Galaburda AM, Corsiglia J, Rosen GD, Sherman GF. Planum temporale asymmetry: Reappraisal since Geschwind and Levitsky. Neuropsychologia. 1987; 25(6):853–868.

Geschwind N. Disconnexion syndromes in animals and man. I. Brain. 1965; 88(2):237–294. [PubMed: 5318481]

Geschwind, N., Galaburda, AM. Cerebral lateralization: biological mechanisms, associations and pathology. Cambridge, MA: MIT Press; 1987.

Goldman-Rakic PS. Topography of cognition: parallel distributed networks in primate association cortex. Annu Rev Neurosci. 1988; 11:137–156. [PubMed: 3284439]

Gorno-Tempini ML, Hillis AE, Weintraub S, Kertesz A, Mendez M, Cappa SF, et al. Classification of primary progressive aphasia and its variants. Neurology. 2011; 76(11):1006–1014. DOI: 10.1212/WNL.0b013e31821103e6 [PubMed: 21325651]

Gow DW Jr, Keller CJ, Eskandar E, Meng N, Cash SS. Parallel versus serial processing dependencies in the perisylvian speech network: a Granger analysis of intracranial EEG data. Brain Lang. 2009; 110(1):43–48. [PubMed: 19356793]

Gow DW Jr, Segawa JA, Ahlfors SP, Lin FH. Lexical influences on speech perception: a Granger causality analysis of MEG and EEG source estimates. Neuroimage. 2008; 43(3):614–623. [PubMed: 18703146]

Heid O. Eddy current-nulled diffusion weighting. Proc Intl Soc Mag Reson Med. 2000; 8:799.

Heilman KM, Pandya DN, Geschwind N. Trimodal inattention following parietal lobe ablations. Trans Am Neurol Assoc. 1970; 95:259–261. [PubMed: 4998763]

Heilman, KM., Valenstein, E. Clinical neuropsychology. New York: Oxford University Press; 1985.

Heilman KM, Van Den Abell T. Right hemisphere dominance for attention: the mechanism underlying hemispheric asymmetries of inattention (neglect). Neurology. 1980; 30(3):327–330. [PubMed: 7189037]

Heilman KM, Watson RT, Bower D, Valenstein E. Right hemisphere dominance for attention. Rev Neurol (Paris). 1983; 139(1):15–17. [PubMed: 6407086]

Hickok G. Functional anatomy of speech perception and speech production: psycholinguistic implications. J Psycholinguist Res. 2001; 30(3):225–235. [PubMed: 11523272]

Hickok G, Poeppel D. Towards a functional neuroanatomy of speech perception. Trends Cogn Sci. 2000; 4(4):131–138. [PubMed: 10740277]

Hickok G, Poeppel D. The cortical organization of speech processing. Nat Rev Neurosci. 2007; 8(5): 393–402. [PubMed: 17431404]

Jenkinson M, Smith S. A global optimisation method for robust affine registration of brain images. Med Image Anal. 2001; 5(2):143–156. [PubMed: 11516708]

Kamali A, Flanders AE, Brody J, Hunter JV, Hasan KM. Tracing superior longitudinal fasciculus connectivity in the human brain using high resolution diffusion tensor tractography. Brain Struct Funct. 2014a; 219(1):269–281. DOI: 10.1007/s00429-012-0498-y [PubMed: 23288254]

Kamali A, Sair HI, Radmanesh A, Hasan KM. Decoding the superior parietal lobule connections of the superior longitudinal fasciculus/arcuate fasciculus in the human brain. Neuroscience. 2014b; 277:577–583. DOI: 10.1016/j.neuroscience.2014.07.035 [PubMed: 25086308]

Karnath HO, Ferber S, Himmelbach M. Spatial awareness is a function of the temporal not the posterior parietal lobe. Nature. 2001; 411(6840):950–953. [PubMed: 11418859]

Kasai K, Shenton ME, Salisbury DF, Hirayasu Y, Lee CU, Ciszewski AA, et al. Progressive decrease of left superior temporal gyrus gray matter volume in patients with first-episode schizophrenia. Am J Psychiatry. 2003; 160(1):156–164. [PubMed: 12505815]

Kellmeyer P, Ziegler W, Peschke C, Juliane E, Schnell S, Baumgaertner A, et al. Fronto-parietal dorsal and ventral pathways in the context of different linguistic manipulations. Brain Lang. 2013; 127(2):241–250. DOI: 10.1016/j.bandl.2013.09.011 [PubMed: 24183468]

Klingberg T, Hedehus M, Temple E, Salz T, Gabrieli JD, Moseley ME, et al. Microstructure of temporo-parietal white matter as a basis for reading ability: evidence from diffusion tensor magnetic resonance imaging. Neuron. 2000; 25(2):493–500. [PubMed: 10719902]

Lacquaniti F, Guigon E, Bianchi L, Ferraina S, Caminiti R. Representing spatial information for limb movement: role of area 5 in the monkey. Cereb Cortex. 1995; 5(5):391–409. [PubMed: 8547787]

Le Bihan D, Breton E, Lallemand D, Grenier P, Cabanis E, Laval-Jeantet M. MR imaging of intravoxel incoherent motions: application to diffusion and perfusion in neurologic disorders. Radiology. 1986; 161(2):401–407. DOI: 10.1148/radiology.161.2.3763909 [PubMed: 3763909]

Lori NF, Akbudak E, Shimony JS, Cull TS, Snyder AZ, Guillory RK, et al. Diffusion tensor fiber tracking of human brain connectivity: aquisition methods, reliability analysis and biological results. NMR Biomed. 2002; 15(7–8):494–515. [PubMed: 12489098]

Ludwig, E., Klingler, J. Atlas cerebri humani. Der innere Bau des Gehirns dargestellt auf Grund makroskopischer Präparate. The inner structure of the brain demonstrated on the basis of macroscopical preparations. Boston: Little, Brown; 1956.

Luria, AR. Higher cortical functions in man. 2. New York: Consultants Bureau; 1980.

Makris, N. Doctoral thesis. Boston University; Boston, MA: 1999. Delineation of human assocation fiber pathways using histologic and magnetic resonance methodologies.

Makris N, Biederman J, Valera EM, Bush G, Kaiser J, Kennedy DN, et al. Cortical thinning of the attention and executive function networks in adults with attention-deficit/hyperactivity disorder. Cereb Cortex. 2007a; 17(6):1364–1375. [PubMed: 16920883]

Makris N, Buka SL, Biederman J, Papadimitriou GM, Hodge SM, Valera EM, et al. Attention and executive systems abnormalities in adults with childhood ADHD: A DT-MRI study of connections. Cereb Cortex. 2008; 18(5):1210–1220. DOI: 10.1093/cercor/bhm156 [PubMed: 17906338]

Makris N, Kennedy DN, McInerney S, Sorensen AG, Wang R, Caviness VS Jr, et al. Segmentation of subcomponents within the superior longitudinal fascicle in humans: a quantitative, in vivo, DT-MRI study. Cereb Cortex. 2005; 15(6):854–869. [PubMed: 15590909]

Makris N, Meyer JW, Bates JF, Yeterian EH, Kennedy DN, Caviness VS. MRI-Based topographic parcellation of human cerebral white matter and nuclei II. Rationale and applications with systematics of cerebral connectivity. Neuroimage. 1999; 9(1):18–45. [PubMed: 9918726]

Makris N, Pandya DN. The extreme capsule in humans and rethinking of the language circuitry. Brain Struct Funct. 2009; 213(3):343–358. [PubMed: 19104833]

Makris N, Pandya DN, Normandin JJ. Quantitative DT-MRI investigations of the human cingulum bundle. Central Nervous System Spectrums. 2002a; 7(7):522–528.

Makris N, Papadimitriou GM, Kaiser JR, Sorg S, Kennedy DN, Pandya DN. Delineation of the middle longitudinal fascicle in humans: a quantitative, in vivo, DT-MRI study. Cereb Cortex. 2009; 19(4): 777–785. DOI: 10.1093/cercor/bhn124 [PubMed: 18669591]

Makris N, Papadimitriou GM, Sorg S, Kennedy DN, Caviness VS, Pandya DN. The occipitofrontal fascicle in humans: a quantitative, in vivo, DT-MRI study. Neuroimage. 2007b; 37(4):1100–1111. DOI: 10.1016/j.neuroimage.2007.05.042 [PubMed: 17681797]

Makris, N., Papadimitriou, GM., Worth, AJ., Jenkins, BG., Garrido, L., Sorensen, AG., et al. Diffusion tensor imaging. In: Nemeroff, C., editor. Neuropsychopharmacology: the fifth generation of progress. Vol. 3. New York: Lippincott, Williams, and Wilkins; 2002b. p. 357-371.Chapter 27

Makris N, Preti MG, Asami T, Pelavin P, Campbell B, Papadimitriou GM, et al. Human middle longitudinal fascicle: variations in patterns of anatomical connections. Brain Struct Funct. 2013a; 218(4):951–968. DOI: 10.1007/s00429-012-0441-2 [PubMed: 22782432]

Makris N, Preti MG, Wassermann D, Rathi Y, Papadimitriou GM, Yergatian C, et al. Human middle longitudinal fascicle: segregation and behavioral-clinical implications of two distinct fiber connections linking temporal pole and superior temporal gyrus with the angular gyrus or superior parietal lobule using multi-tensor tractography. Brain Imaging Behav. 2013b; 7(3):335–352. DOI: 10.1007/s11682-013-9235-2 [PubMed: 23686576]

Makris N, Rathi Y, Mouradian P, Bonmassar G, Papadimitriou G, Ing WI, et al. Variability and anatomical specificity of the orbitofrontothalamic fibers of passage in the ventral capsule/ventral striatum (VC/VS): precision care for patient-specific tractography-guided targeting of deep brain stimulation (DBS) in obsessive compulsive disorder (OCD). Brain Imaging Behav. 2015; doi: 10.1007/s11682-015-9462-9

Makris N, Seidman LJ, Ahern T, Kennedy DN, Caviness VS, Tsuang MT, et al. White matter volume abnormalities and associations with symptomatology in schizophrenia. Psychiatry Res. 2010; 183(1):21–29. DOI: 10.1016/j.pscychresns.2010.04.016 [PubMed: 20538438]

Makris N, Worth AJ, Sorensen AG, Papadimitriou GM, Wu O, Reese TG, et al. Morphometry of in vivo human white matter association pathways with diffusion-weighted magnetic resonance imaging. Ann Neurol. 1997; 42(6):951–962. [PubMed: 9403488]

Malcolm JG, Shenton ME, Rathi Y. Filtered multitensor tractography. IEEE Trans Med Imaging. 2010; 29(9):1664–1675. DOI: 10.1109/TMI.2010.2048121 [PubMed: 20805043]

Maldonado IL, de Champfleur NM, Velut S, Destrieux C, Zemmoura I, Duffau H. Evidence of a middle longitudinal fasciculus in the human brain from fiber dissection. J Anat. 2013; 223(1):38–45. DOI: 10.1111/joa.12055 [PubMed: 23621438]

Martino J, da Silva-Freitas R, Caballero H, Marco de Lucas E, Garcia-Porrero JA, Vazquez-Barquero A. Fiber dissection and diffusion tensor imaging tractography study of the temporoparietal fiber intersection area. Neurosurgery. 2013; 72(1 Suppl Operative):87–97. discussion 97–88. DOI: 10.1227/NEU.0b013e318274294b [PubMed: 23417154]

Men jot de Champfleur N, Lima Maldonado I, Moritz-Gasser S, Machi P, Le Bars E, Bonafe A, et al. Middle longitudinal fasciculus delineation within language pathways: a diffusion tensor imaging study in human. Eur J Radiol. 2013; 82(1):151–157. DOI: 10.1016/j.ejrad.2012.05.034 [PubMed: 23084876]

Mesulam MM. Tetramethyl benzidine for horseradish peroxidase neurohistochemistry: a non-carcinogenic blue reaction product with superior sensitivity for visualizing neural afferents and efferents. J Histochem Cytochem. 1978; 26(2):106–117. [PubMed: 24068]

Mesulam MM. Large-scale neurocognitive networks and distributed processing for attention, language, and memory. Ann Neurol. 1990; 28(5):597–613. [PubMed: 2260847]

Mesulam MM. From sensation to cognition. Brain. 1998; 121(Pt 6):1013–1052. [PubMed: 9648540]

Mesulam MM, Thompson CK, Weintraub S, Rogalski EJ. The Wernicke conundrum and the anatomy of language comprehension in primary progressive aphasia. Brain. 2015; 138(Pt 8):2423–2437. DOI: 10.1093/brain/awv154 [PubMed: 26112340]

Meynert, T. Leidesdorf's Lehrbuch der phychischen Krankheiten. Erlangen: 1865. Anatomie der Hirnrinde und ihre Verbindungsbahnen mit den empfindenden Oberflachen und den bewegenden Massen.

Molholm S, Sehatpour P, Mehta AD, Shpaner M, Gomez-Ramirez M, Ortigue S, et al. Audio-visual multisensory integration in superior parietal lobule revealed by human intracranial recordings. J Neurophysiol. 2006; 96(2):721–729. [PubMed: 16687619]

Mori S, Crain BJ, Chacko VP, van Zijl PC. Three-dimensional tracking of axonal projections in the brain by magnetic resonance imaging. Ann Neurol. 1999; 45(2):265–269. [PubMed: 9989633]

Mountcastle VB, Lynch JC, Georgopoulos A, Sakata H, Acuna C. Posterior parietal association cortex of the monkey: command functions for operations within extrapersonal space. J Neurophysiol. 1975; 38(4):871–908. [PubMed: 808592]

Pandya, DN., Yeterian, EH. Architecture and connections of cortical association areas. In: Peters, A., Jones, EG., editors. Cerebral cortex: association and auditory areas. Vol. 4. New York: Plenum; 1985. p. 3-61.

Petkov CI, Kayser C, Steudel T, Whittingstall K, Augath M, Logothetis NK. A voice region in the monkey brain. Nat Neurosci. 2008; 11(3):367–374. DOI: 10.1038/nn2043 [PubMed: 18264095]

Pierpaoli C, Basser PJ. Toward a quantitative assessment of diffusion anisotropy. Magn Reson Med. 1996; 36(6):893–906. [PubMed: 8946355]

Poremba A, Saunders RC, Crane AM, Cook M, Sokoloff L, Mishkin M. Functional mapping of the primate auditory system. Science. 2003; 299(5606):568–572. [PubMed: 12543977]

Posner MI, Petersen SE. The attention system of the human brain. Annu Rev Neurosci. 1990; 13:25–42. [PubMed: 2183676]

Rajarethinam R, Sahni S, Rosenberg DR, Keshavan MS. Reduced superior temporal gyrus volume in young offspring of patients with schizophrenia. Am J Psychiatry. 2004; 161(6):1121–1124. [PubMed: 15169705]

Rascovsky K, Hodges JR, Knopman D, Mendez MF, Kramer JH, Neuhaus J, et al. Sensitivity of revised diagnostic criteria for the behavioural variant of frontotemporal dementia. Brain. 2011; 134(Pt 9):2456–2477. DOI: 10.1093/brain/awr179 [PubMed: 21810890]

Rathi Y, Malcolm JG, Bouix S, Westin CF, Shenton ME. False positive detection using filtered tractography. Proc Intl Soc Mag Reson Med. 2010; 18:4019.

Rauschecker JP, Tian B. Mechanisms and streams for processing of "what" and "where" in auditory cortex. Proc Natl Acad Sci U S A. 2000; 97(22):11800–11806. DOI: 10.1073/pnas.97.22.11800 [PubMed: 11050212]

Reil, DJC., Autenrieth, DJHF. Archiv fur die Physiologie. Halle: In Der Curtschen Buchhandlung; 1809.

Rilling JK, Glasser MF, Preuss TM, Ma X, Zhao T, Hu X, et al. The evolution of the arcuate fasciculus revealed with comparative DTI. Nat Neurosci. 2008; 11(4):426–428. DOI: 10.1038/nn2072 [PubMed: 18344993]

Sakata H, Takaoka Y, Kawarasaki A, Shibutani H. Somatosensory properties of neurons in the superior parietal cortex (area 5) of the rhesus monkey. Brain Res. 1973; 64:85–102. [PubMed: 4360893]

Sapolsky D, Bakkour A, Negreira A, Nalipinski P, Weintraub S, Mesulam MM, et al. Cortical neuroanatomic correlates of symptom severity in primary progressive aphasia. Neurology. 2010; 75(4):358–366. [PubMed: 20660866]

Schmahmann, JD., Pandya, DN. Fiber pathways of the brain. New York: Oxford University Press; 2006.

Seltzer B, Pandya DN. Afferent cortical connections and architectonics of the superior temporal sulcus and surrounding cortex in the rhesus monkey. Brain Res. 1978; 149(1):1–24. [PubMed: 418850]

Seltzer B, Pandya DN. Further observations on parieto-temporal connections in the rhesus monkey. Exp Brain Res. 1984; 55(2):301–312. [PubMed: 6745368]

Seltzer B, Pandya DN. Post-rolandic cortical projections of the superior temporal sulcus in the rhesus monkey. J Comp Neurol. 1991; 312(4):625–640. [PubMed: 1761745]

Song SK, Sun SW, Ju WK, Lin SJ, Cross AH, Neufeld AH. Diffusion tensor imaging detects and differentiates axon and myelin degeneration in mouse optic nerve after retinal ischemia. Neuroimage. 2003; 20(3):1714–1722. [PubMed: 14642481]

Song SK, Sun SW, Ramsbottom MJ, Chang C, Russell J, Cross AH. Dysmyelination revealed through MRI as increased radial (but unchanged axial) diffusion of water. Neuroimage. 2002; 17(3): 1429–1436. [PubMed: 12414282]

Suchan J, Umarova R, Schnell S, Himmelbach M, Weiller C, Karnath HO, et al. Fiber pathways connecting cortical areas relevant for spatial orienting and exploration. Hum Brain Mapp. 2014; 35(3):1031–1043. DOI: 10.1002/hbm.22232 [PubMed: 23283834]

Talairach, J., Tournoux, P. Co-planar stereotaxic atlas of the human brain. New York: Thieme Medical Publishers, Inc; 1988.

Thiebaut de Schotten M, Dell'Acqua F, Forkel SJ, Simmons A, Vergani F, Murphy DG, et al. A lateralized brain network for visuospatial attention. Nat Neurosci. 2011; 14(10):1245–1246. [PubMed: 21926985]

Tian B, Reser D, Durham A, Kustov A, Rauschecker JP. Functional specialization in rhesus monkey auditory cortex. Science. 2001; 292(5515):290–293. DOI: 10.1126/science.1058911 [PubMed: 11303104]

Tuch DS, Reese TG, Wiegell MR, Makris N, Belliveau JW, Wedeen VJ. High angular resolution diffusion imaging reveals intravoxel white matter fiber heterogeneity. Magn Reson Med. 2002; 48(4):577–582. [PubMed: 12353272]

Turken AU, Dronkers NF. The neural architecture of the language comprehension network: converging evidence from lesion and connectivity analyses. Front Syst Neurosci. 2011; 5:1. [PubMed: 21347218]

Wang Y, Fernandez-Miranda JC, Verstynen T, Pathak S, Schneider W, Yeh FC. Rethinking the role of the middle longitudinal fascicle in language and auditory pathways. Cereb Cortex. 2013; 23(10): 2347–2356. DOI: 10.1093/cercor/bhs225 [PubMed: 22875865]

Watson RT, Valenstein E, Day A, Heilman KM. Posterior neocortical systems subserving awareness and neglect. Neglect associated with superior temporal sulcus but not area 7 lesions. Arch Neurol. 1994; 51(10):1014–1021. [PubMed: 7944999]

Wernicke, C. Der aphasiche Symptomenkomplex. Breslau: Cohn und Weigert; 1874.

Whitwell JL, Weigand SD, Boeve BF, Senjem ML, Gunter JL, DeJesus-Hernandez M, et al. Neuroimaging signatures of frontotemporal dementia genetics: C9ORF72, tau, progranulin and sporadics. Brain. 2012; 135(Pt 3):794–806. DOI: 10.1093/brain/aws001 [PubMed: 22366795]

Wolk DA, Dickerson BC. Alzheimer's Disease Neuroimaging I. Apolipoprotein E (APOE) genotype has dissociable effects on memory and attentional-executive network function in Alzheimer's disease. Proc Natl Acad Sci U S A. 2010; 107(22):10256–10261. DOI: 10.1073/pnas.1001412107 [PubMed: 20479234]

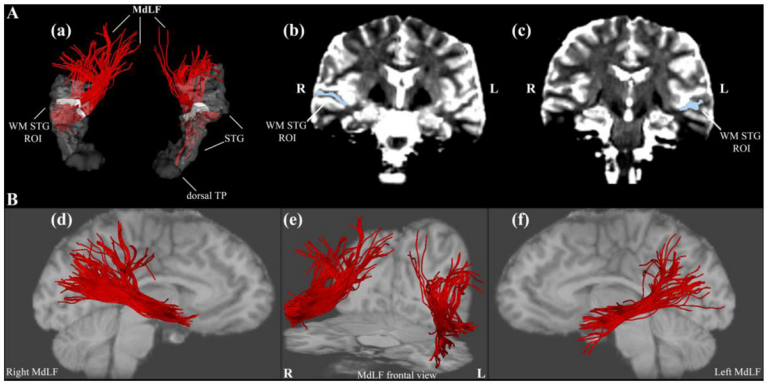

Figure 1.

Figure 1A: Method of tractography of the middle longitudinal fascicle (MdLF) shown in a single subject. A critical component for the delineation of MdLF (a, in red) is the use of a white matter (WM) region of interest (ROI, in white) as a seed in the core of the superior temporal gyrus (STG) white matter of the right (R) and left (L) hemispheres in the coronal plane (b, c). This WM ROI is composed of all WM voxels of the STG at a single coronal level corresponding to Y = −13 mm in the anterior-posterior dimension of the Talairach stereotaxic coordinate system (Talairach and Tournoux 1988) as elaborated upon in Methods. **B:** Representations of MdLF (in red) in the right hemisphere in lateral view (d), in both hemispheres in frontal view (e), and in the left hemisphere in lateral view (f). Abbreviations: L = left; R = right; TP = temporal pole.

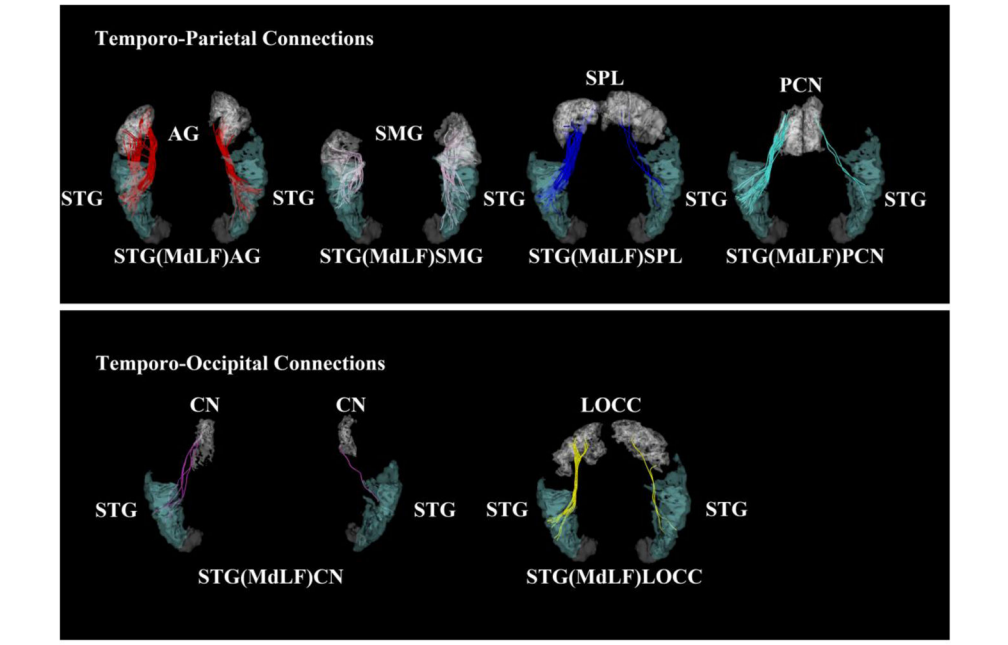

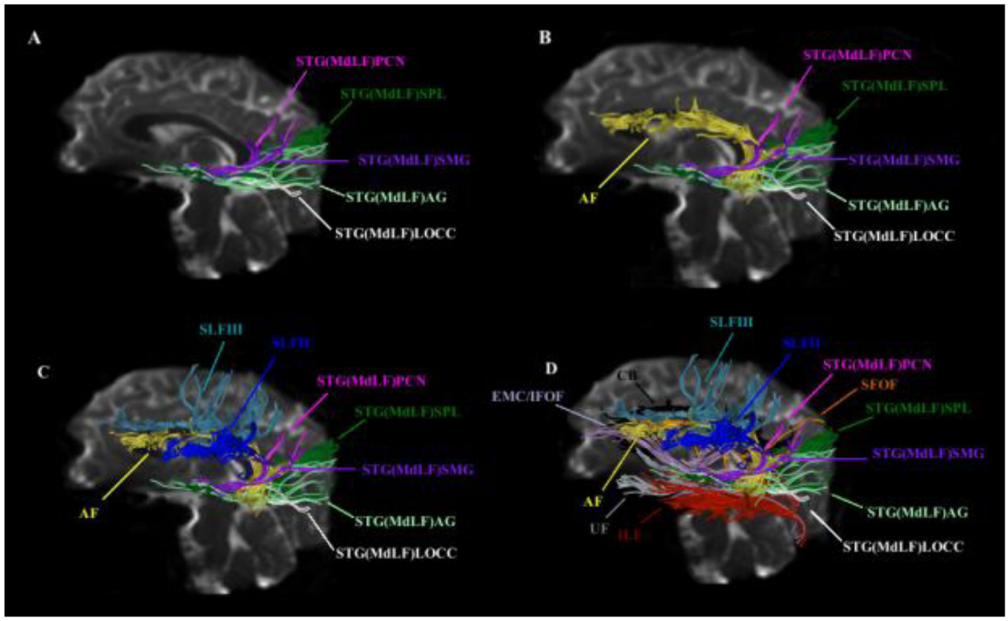

Figure 2.

Method of tractography of the middle longitudinal fascicle (MdLF) (continued). Another element for the delineation of MdLF is the use of cortical regions of interest (ROIs) of origin and termination. The different connections within the MdLF have been determined by connecting selectively the superior temporal gyrus and temporopolar cortex (STG) with four parietal ROIs (shown in upper diagrams), namely angular gyrus (AG), supramarginal gyrus (SMG), superior parietal lobule (SPL), and precuneus (PCN), and with two occipital cortical ROIs (shown in lower diagrams), i.e., the cuneus (CN) and the lateral occipital area (LOCC). The cortical ROIs have been segmented using FreeSurfer and the tracing done using the

white matter query language (WMQL) software as elaborated upon in Methods. Temporo-parietal connections (upper diagrams) comprise the superior temporal-angular gyrus, STG(MdLF)AG; superior temporal-supramarginal gyrus, STG(MdLF)SMG; superior temporal-superior parietal lobule, STG(MdLF)SPL; and superior temporal-precuneus, STG(MdLF)PCN, fiber tracts, whereas temporo-occipital connections (lower diagrams) include the superior temporal-cuneus, STG(MdLF)CN, and superior temporal-lateral occipital, STG(MdLF)LOCC, fiber tracts.

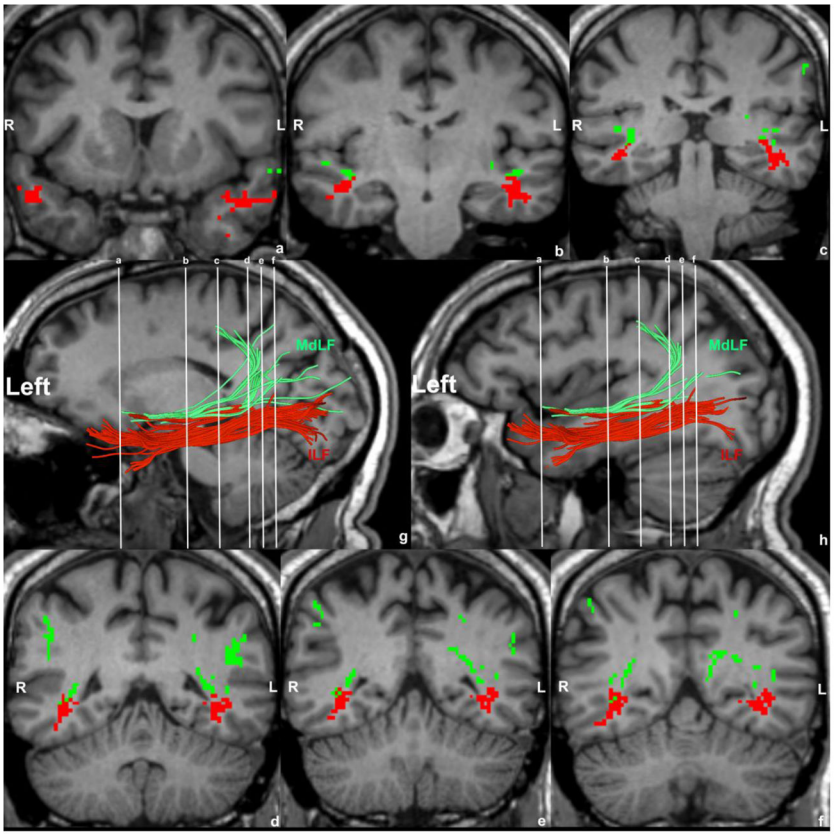

Figure 3.

Figure 3A: Delineation of temporo-parietal and temporo-occipital connections of the human MdLF shown in a single subject (A) and their distinction from other long association cortico-cortical fiber tracts such as the arcuate fascicle (AF, in yellow, B), superior longitudinal fascicles II (SLF II, in dark blue, C) and III (SLF III, in light blue, C), uncinate fascicle (UF, in grey, D), inferior longitudinal fascicle (ILF, in red, D), superior fronto-occipital fascicle (SFOF, in orange, D), cingulum bundle (CB, in black, D) and the extreme capsule/inferior occipitofrontal fascicle complex (EMC/IFOF, in light purple, D). MdLF's connections are temporo-parietal such as the superior temporal-angular gyrus (STG(MdLF)AG, in light green), superior temporal-supramarginal gyrus (STG(MdLF)SMG, in dark purple), superior temporal-superior parietal lobule (STG(MdLF)SPL, in dark green), superior temporal-precuneus (STG(MdLF)PCN, in pink) and temporo-occipital such as the superior temporal-cuneus (STG(MdLF)CN, not shown in this figure) and superior temporal-lateral occipital (STG(MdLF)LOCC, in white). **B:** Illustrative comparison of MdLF (in green) and ILF (in red) in the left and right hemispheres of a single subject in the coronal (a–f) sagittal (g, h, left hemisphere only) planes. Abbreviations: L, left hemisphere; R, right hemisphere.

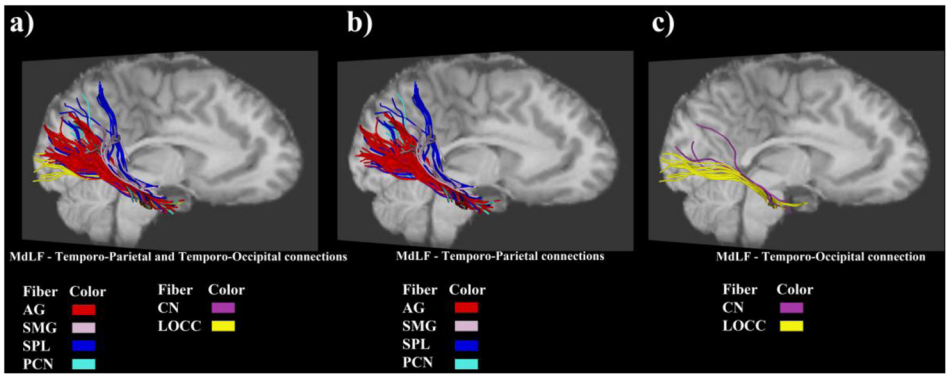

Figure 4.

Results of four temporo-parietal and two temporo-occipital connections (a) of the human MdLF with color-coding scheme, shown in a single subject. Temporo-parietal connections (b) are the superior temporal-angular gyrus, STG(MdLF)AG; superior temporal-supramarginal gyrus, STG(MdLF)SMG; superior temporal-superior parietal lobule, STG(MdLF)SPL; and superior temporal-precuneus, STG(MdLF)PCN, fiber tracts, whereas temporo-occipital connections (c) include the superior temporal-cuneus, STG(MdLF)CN, and superior temporal-lateral occipital, STG(MdLF)LOCC, fiber tracts.

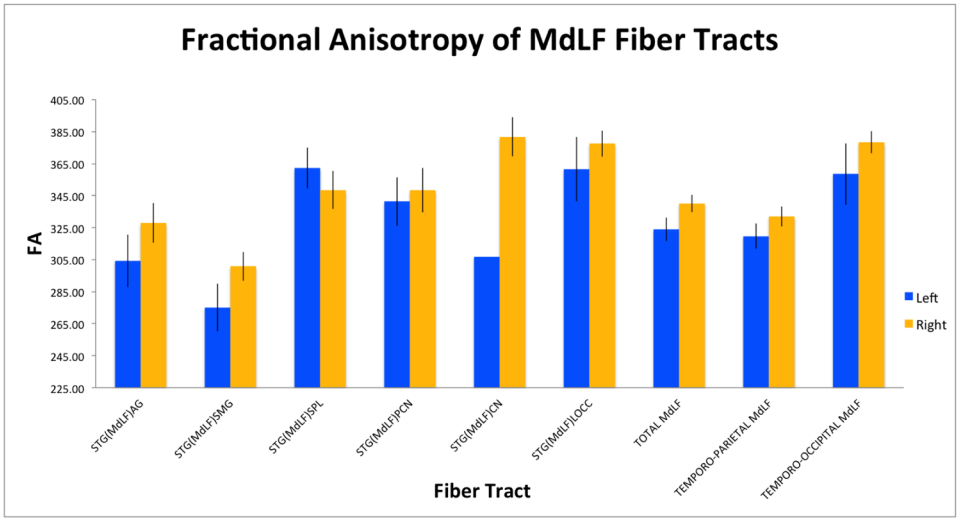

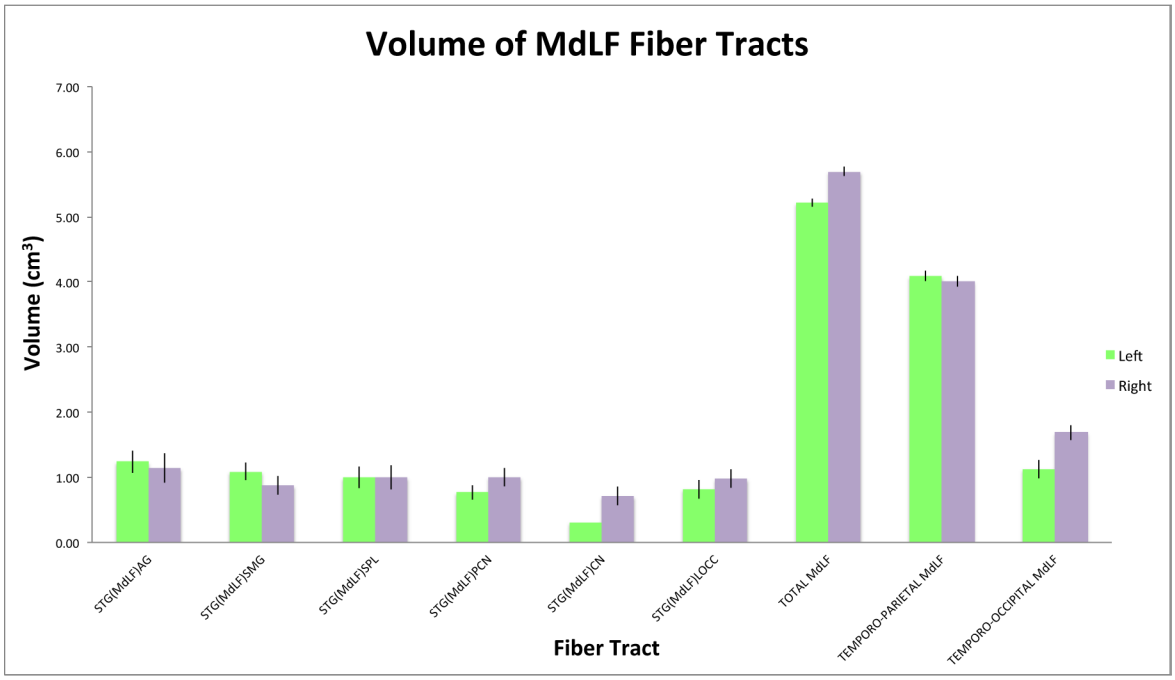

Figure 5.

Graphical representations of the fractional anisotropy **(A)** and volume **(B)** of six left and right fiber connections of the human middle longitudinal fascicle (MdLF) in 70 healthy subjects, based on the data in Table 1. Four of these connections are temporo-parietal: superior temporal-angular gyrus, STG(MdLF)AG; superior temporal-supramarginal, STG(MdLF)SMG; superior temporal-superior parietal lobule, STG(MdLF)SPL; and superior temporal-precuneus, STG(MdLF)PCN. The two temporo-occipital conections are the superior temporal-cuneus, STG(MdLF)CN, and superior temporal-lateral occipital, STG(MdLF)LOCC.

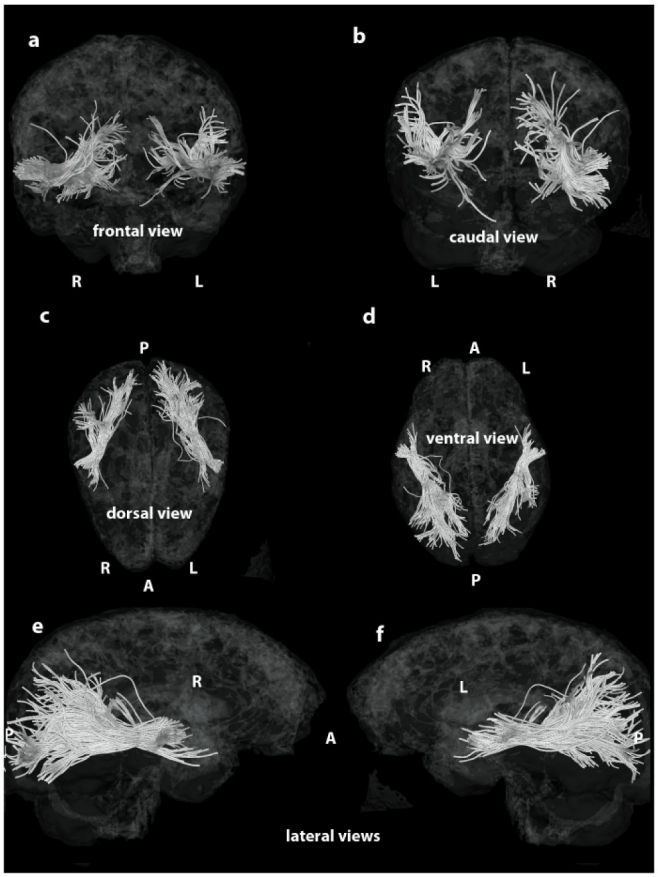

Figure 6.

Depiction of the MdLF mapped onto a semitransparent 3-D reconstruction of the MNI brain: a, frontal view; b caudal view; c, dorsal view; d, ventral view; e, f, lateral views. Abbreviations: A, anterior; P, posterior; L, left hemisphere; R, right hemisphere.

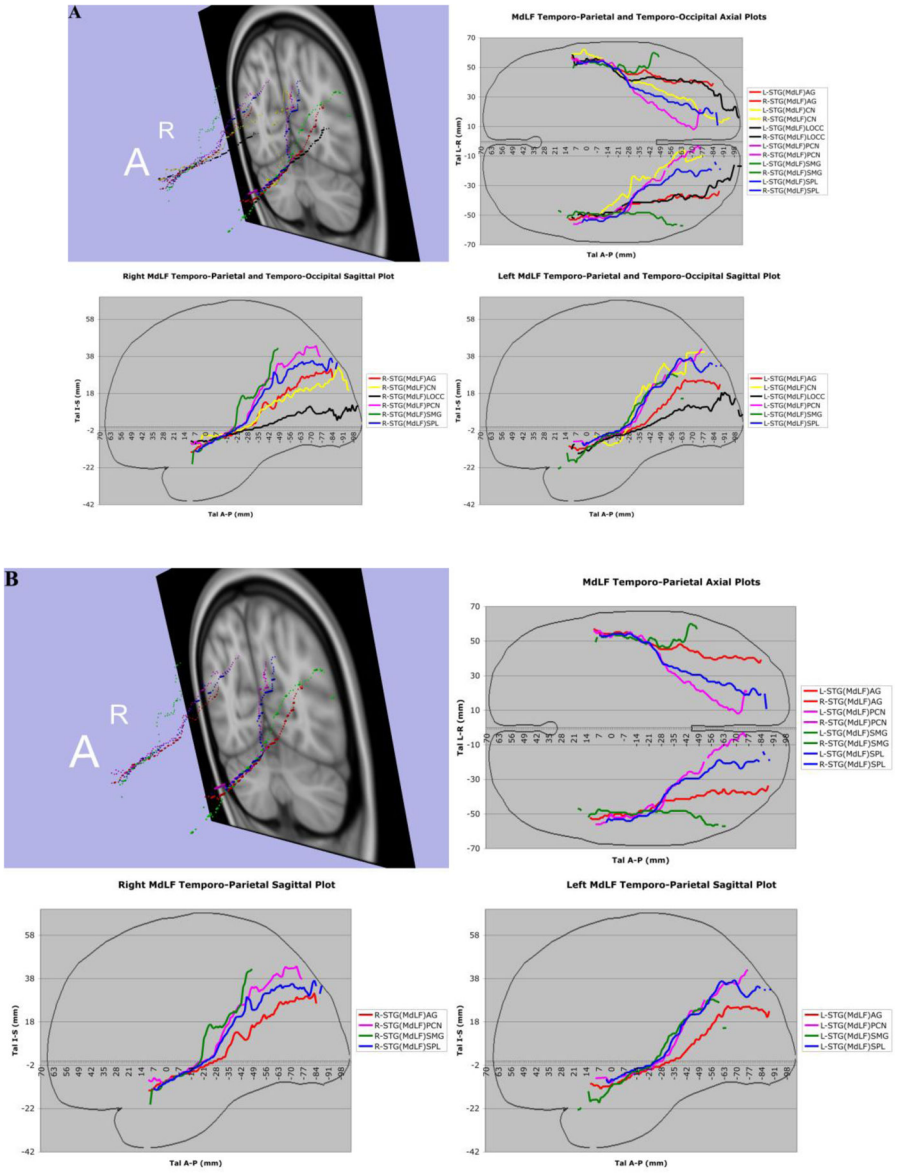

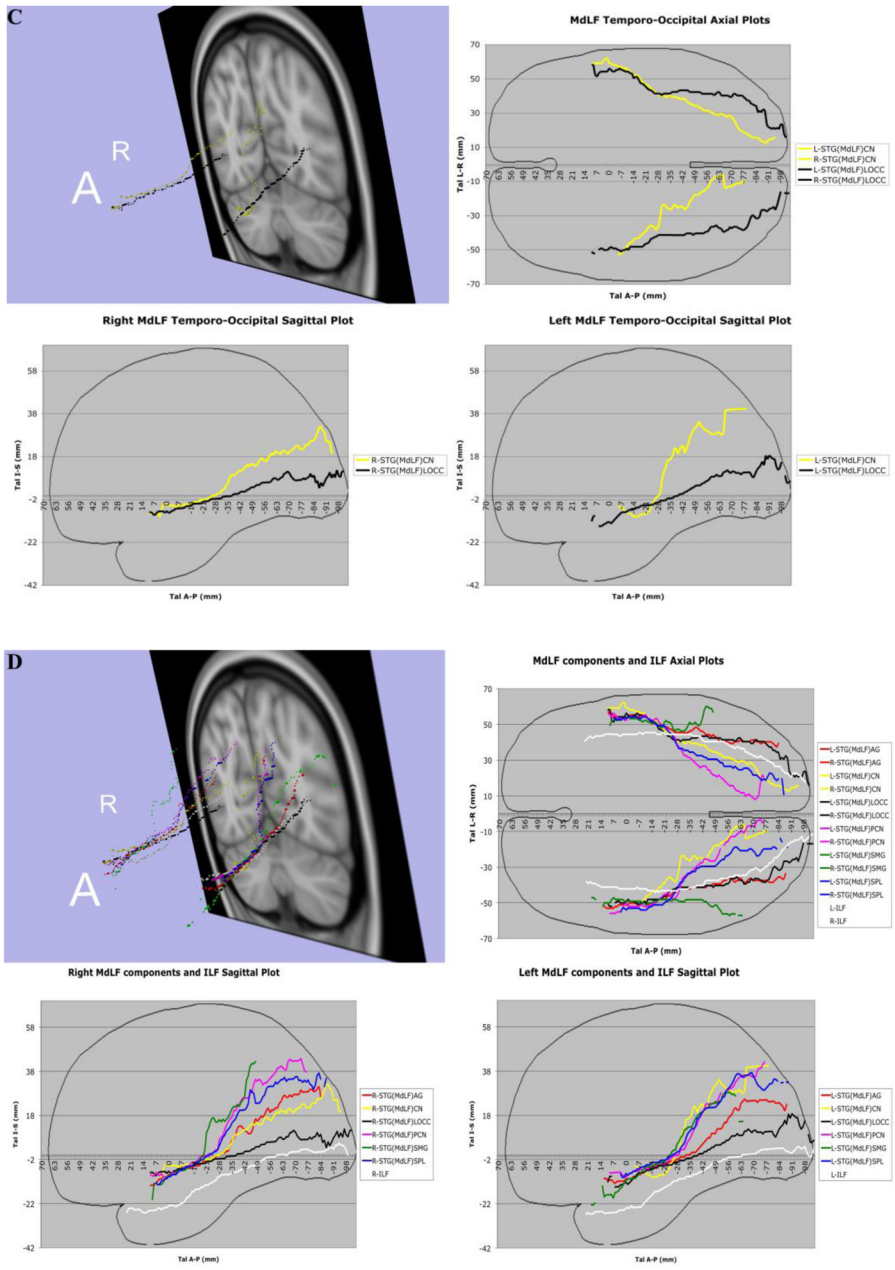

Figure 7.

In **7A**, the complete trajectories of the temporo-parietal and temporo-occipital subdivisions of the human middle longitudinal fascicle (MdLF), represented as a center of mass line (Makris et al., 2013), of the 70 subjects of this study have been placed in the Talairach coordinate space. The MdLF connections are temporo-parietal, such as the superior temporal-angular gyrus, STG(MdLF)AG; superior temporal-supramarginal gyrus, STG(MdLF)SMG; superior temporal-superior parietal lobule, STG(MdLF)SPL; superior temporal-precuneus STG(MdLF)PCN; and temporo-occipital, such as the superior temporal-cuneus, STG(MdLF)CN, and superior temporal-lateral occipital, STG(MdLF)LOCC. In **7B**, the complete trajectories of the temporo-parietal subdivisions of the human middle

longitudinal fascicle (MdLF), represented as a center of mass line, of the 70 subjects of this study have been placed in the Talairach coordinate space. The temporo-parietal connections are the superior temporal-angular gyrus, STG(MdLF)AG; superior temporal-supramarginal gyrus, STG(MdLF)SMG; superior temporal-superior parietal lobule, STG(MdLF)SPL, and superior temporal-precuneus, STG(MdLF)PCN, fiber tracts. In **7C**, the average of the complete trajectories, represented as a center of mass line, of the two temporo-occipital subdivisions of the human middle longitudinal fascicle (MdLF) of the 70 subjects of this study has been placed in the Talairach coordinate space. These connections are the superior temporal-cuneus, STG(MdLF)CN, and superior temporal-lateral occipital, STG(MdLF)LOCC, fiber tracts. In **7D**, the averages of the complete trajectories, represented as a center of mass line, of the two temporo-occipital subdivisions of the human middle longitudinal fascicle (MdLF) and of the inferior longitudinal fascicle (ILF) of the 70 subjects of this study have been placed in the Talairach coordinate space for the purpose of comparison. Abbreviations: A = anterior; A–P = anterior-posterior; L = left; R = right; Tal = Talairach coordinate space.

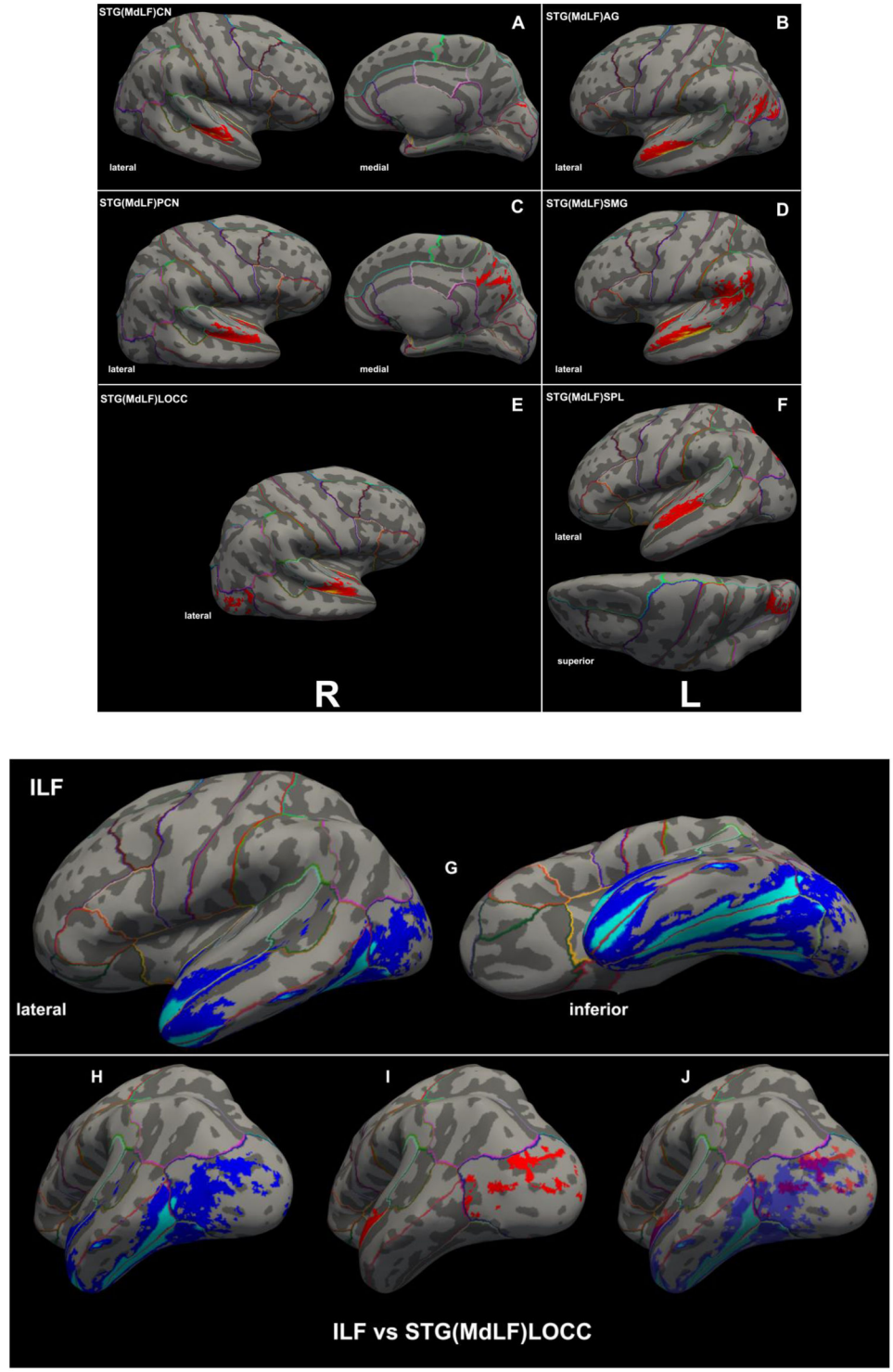

Figure 8.

Figure 8A–F. Cortical representations (in red) associated with each of the six branches of MdLF on brain surfaces as determined by FreeSurfer in a template brain, depicted on the left (L) or right (R) hemispheres. The probabilistic maps are average (across representations)

tract representations overlaid onto the MNI template brain. The tract terminations of each MdLF branch were projected on the inflated brain surface (generated using FreeSurfer) of the MNI brain. In **8G–J**, the ILF (in dark and light blue) is similarly shown for the purpose of comparison with the MdLF (in red) branches. It should be noted that the only branch of MdLF sharing common space with ILF is STG(MdLF)LOCC.

Table 1

Measures of volume, fractional anisotropy (FA), axial diffusivity (AD), radial diffusivity (RD), and length of six left and right fiber connections of the human middle longitudinal fascicle (MdLF) in 70 healthy subjects. Four of these connections are temporo-parietal: superior temporal-angular gyrus, STG(MdLF)AG; superior temporal-supramarginal gyrus, STG(MdLF)SMG; superior temporal-superior parietal lobule, STG(MdLF)SPL; and superior temporal-precuneus, STG(MdLF)PCN. The other two temporo-occipital connections are the superior temporal-cuneus, STG(MdLF)CN, and superior temporal-lateral occipital, STG(MdLF)LOCC. Symmetry index (SI) of these parameters is also reported herein. The results in this table are represented graphically in Figure 5.

	Volume (cm^3)			**FA**			**AD**			**RD**			**Length (mm)**		
STG(MdLF)AG	Left	Right	SI	Left	Right	SI	Left	Right	SI	Left	Right	SI	Left	Right	SI
Mean	1.24	1.14	0.09	304.21	327.88	−0.07	1962.57	2093.05	−0.06	1077.44	1146.63	−0.06	84.10	87.11	−0.04
STD	1.10	1.40	−0.24	104.68	77.29	0.30	632.88	462.21	0.31	356.56	265.02	0.29	10.41	9.40	0.10
STG(MdLF)SMG	Left	Right	SI	Left	Right	SI	Left	Right	SI	Left	Right	SI	Left	Right	SI
Mean	1.09	0.87	0.22	275.12	300.82	−0.09	2003.54	2168.48	−0.08	1194.63	1287.50	−0.07	68.44	68.90	−0.01
STD	0.84	0.80	0.05	90.69	51.24	0.56	617.75	292.04	0.72	369.87	176.35	0.71	10.52	15.24	−0.37
STG(MdLF)SPL	Left	Right	SI	Left	Right	SI	Left	Right	SI	Left	Right	SI	Left	Right	SI
Mean	1.00	1.00	0.00	362.25	348.49	0.04	2169.22	2122.14	0.02	1126.15	1130.23	0.00	96.92	100.36	−0.03
STD	0.96	1.11	−0.15	76.24	70.02	0.09	376.32	367.35	0.02	206.61	239.98	−0.15	9.53	8.44	0.12
STG(MdLF)PCN	Left	Right	SI	Left	Right	SI	Left	Right	SI	Left	Right	SI	Left	Right	SI
Mean	0.77	1.00	−0.26	341.30	348.35	−0.02	2146.22	2138.92	0.00	1153.42	1141.85	0.01	92.44	98.26	−0.06
STD	0.66	0.82	−0.22	90.25	82.66	0.09	492.45	436.56	0.12	269.65	239.92	0.12	7.82	9.37	−0.18
STG(MdLF)CN	Left	Right	SI	Left	Right	SI	Left	Right	SI	Left	Right	SI	Left	Right	SI
Mean	0.308	0.71	−0.79	306.91	381.79	−0.22	2277.26	2402.61	−0.05	1359.35	1260.07	0.08	100.76	105.80	−0.05
STD	0	0.51	−2.00	0.00	30.18	−2.00	0.00	143.77	−2.00	0.00	92.51	−2.00	0	8.97	−2.00
STG(MdLF)LOCC	Left	Right	SI	Left	Right	SI	Left	Right	SI	Left	Right	SI	Left	Right	SI
Mean	0.82	0.98	−0.18	361.47	377.55	−0.04	2354.84	2308.58	0.02	1277.35	1212.99	0.05	86.40	91.33	−0.06
STD	0.61	0.68	−0.12	82.89	40.05	0.70	99.14	105.59	−0.06	143.32	79.77	0.57	18.07	10.97	0.49
TOTAL MdLF	Left	Right	SI	Left	Right	SI	Left	Right	SI	Left	Right	SI	Left	Right	SI
Mean	5.22	5.70	−0.09	323.90	340.09	−0.05	2096.50	2163.62	−0.03	1151.86	1181.95	−0.03	85.47	89.94	−0.05
STD	0.32	0.15	0.77	95.58	70.83	0.30	524.22	370.32	0.34	299.95	221.66	0.30	14.78	15.60	−0.05
TEMPORO-PARIETAL MdLF	Left	Right	SI	Left	Right	SI	Left	Right	SI	Left	Right	SI	Left	Right	SI

	Volume (cm^3)			FA			AD			RD			Length (mm)		
Mean	4.09	4.01	0.02	319.72	331.94	−0.04	2065.81	2128.78	−0.03	1136.15	1173.34	−0.03	85.27	89.03	−0.04
STD	0.20	0.11	0.58	96.55	73.58	0.27	546.20	395.83	0.32	310.39	240.43	0.25	14.43	16.16	−0.11
TEMPORO-OCCIPITAL MdLF	Left	Right	SI	Left	Right	SI	Left	Right	SI	Left	Right	SI	Left	Right	SI
Mean	1.12694	1.68746	−0.40	358.44	378.40	−0.05	2350.53	2327.38	0.01	1281.91	1222.41	0.05	87.20	94.22	−0.08
STD	0.36129	0.19006	0.62	81.43	37.85	0.73	97.90	117.77	−0.18	140.38	83.00	0.51	17.85	12.00	0.39